Copy
RM E55F24

NACA

RESEARCH MEMORANDUM

EXPERIMENTAL INVESTIGATION OF METHODS OF IMPROVING DIFFUSER-EXIT TOTAL-PRESSURE PROFILES FOR A SIDE-INLET MODEL AT MACH NUMBER 3.05

By Thomas G. Piercy and John L. Klann

Lewis Flight Propulsion Laboratory
Cleveland, Ohio

NATIONAL ADVISORY COMMITTEE
FOR AERONAUTICS

WASHINGTON

August 29, 1955

NATIONAL ADVISORY COMMITTEE FOR AERONAUTICS

RESEARCH MEMORANDUM

EXPERIMENTAL INVESTIGATION OF METHODS OF IMPROVING DIFFUSER-EXIT TOTAL-PRESSURE PROFILES FOR A SIDE-INLET MODEL AT MACH NUMBER 3.05

By Thomas G. Piercy and John L. Klann

SUMMARY

Several methods of straightening diffuser-exit total-pressure profiles produced by a typical half-conical double-shock side inlet at a free-stream Mach number of 3.05 were investigated. These methods included the use of (a) longer subsonic diffusers, (b) constant-area mixing sections at the diffuser exit, (c) internal screens, (d) a rapid acceleration of the flow at the diffuser exit, (e) internal bleed, and (f) a change in internal-flow passage shape obtained by raising the internal centerbody fairing from the floor into the diffuser duct.

Each of the methods investigated was found to be effective in reducing distortion. Increasing the model length was found to be quite effective in reducing the total-pressure distortion. In particular, the addition of length through the use of constant-area mixing sections at the end of the diffuser reduced the distortion with little or no loss in pressure recovery. Increasing the basic subsonic diffuser length was also effective, and the longer of two subsonic diffuser models yielded the lower distortion at the diffuser exit.

The use of screens and the change in centerbody location reduced the distortion at the expense of pressure-recovery losses. On the other hand, the use of bleed from the inlet throat or an acceleration of the flow at the diffuser exit reduced the distortion with no loss in pressure recovery.

INTRODUCTION

Large total-pressure distortions have been measured at the diffuser exits of air inlets feeding turbojet and ram-jet engines. Although this problem has been known for some time, only recently has material pertaining to methods of reducing these distortions appeared in the literature. Impetus has been provided by the requirement of flight at higher speeds

and at higher altitudes. Nonuniform flow entering the turbojet engine has necessitated a derating of the engines in order to prevent turbine burn-out and also has limited high-altitude flight because of induced surge and stall phenomenon (e.g., ref. 1).

Causes of flow distortion are somewhat dependent upon flight speed. At subsonic flight speeds air generally enters the inlet with little distortion. Even in this case, however, flow distortions may result when the flow is turned or diffused too rapidly. For example, operation at angle of attack or at large mass-flow ratios may cause local separation from the inlet lip. Inside the diffuser, separation may result from too rapid a diffusion rate or may occur locally in regions where the wall rate of curvature is too large. These separated regions tend to spread as the flow traverses the diffuser. Basically, then, the problem of the diffuser in the subsonic speed range is to maintain the relatively low distortion that exists immediately upstream of the inlet.

In contrast to the subsonic case, flow distortions generally exist at the inlet throat at supersonic flight speeds. These distortions are caused primarily by nonuniform supersonic compression which may occur, for example, because of interaction between the inlet terminal shock and the compression-surface boundary layer, because of operation at reduced mass flow with subsequent entrance of a vortex sheet into the inlet, or because of operation at angle of attack or yaw.

At least two general solutions to the problem of obtaining uniform flow at the diffuser exit are evident. First, means may be employed to provide more uniform flow at the inlet throat. For example, removal of the boundary layer at the inlet throat with an internal scoop or slot should minimize shock - boundary-layer interaction effects. Second, the distorted flow at the inlet throat may be mixed in the subsonic diffuser. In previous investigations (e.g., refs. 2 to 4) mixing in the subsonic diffuser has been forced by the use of such devices as screens, vortex generators, and freely rotating blade rows. Although distortion reduction has been achieved, losses in total-pressure recovery have been suffered.

It might also be expected that increasing the diffuser length would reduce distortion inasmuch as the additional length would aid natural mixing and perhaps incur smaller pressure losses. The present investigation was conducted at the NACA Lewis laboratory to determine the effect of mixing length on total-pressure distortion at the diffuser exit of a typical side inlet at a Mach number of 3.05.

Additional methods of mixing studied for comparison include the use of (1) screens, (2) an acceleration of the flow at the diffuser exit, (3) a change in diffuser flow passage shape, and (4) internal boundary-layer bleed from the inlet throat.

SYMBOLS

The following symbols are used in this report:

A	area
D	diffuser-exit diameter, 2.2 in.
L	length of constant-area mixing section ahead of pressure rake, in.
L/D	constant-area mixing-length parameter
m	mass flow
P	total pressure
P_l	total pressure at individual pressure tubes
ΔP	maximum pressure variation across pressure rake, $\Delta P = P_{l,max} - P_{l,min}$
R	inlet radius, 1.5 in.

Subscripts:

av	average
max	maximum
min	minimum
t	throat
0	free stream
1	conditions at inlet throat
2	conditions at movable (primary) rake

APPARATUS AND PROCEDURE

Tests were conducted in the 18- by 18-inch Mach number 3.05 tunnel. The tunnel test-section temperature was maintained at 150° F, while the total pressure was approximately atmospheric. The dew point of the air was kept at -20° F or lower to minimize condensation effects.

Model. - The model used for these tests was a half-conical side inlet with external compression provided by a 19.8°-34.4° double-shock spike designed to capture a full streamtube of air at a Mach number of 3.05.

Except for modifications to the subsonic diffuser, the model was the same as reported in reference 5. The modifications included (1) a reduction of the diffuser area ratio to provide a more realistic diffuser-exit Mach number for a turbojet engine operating near free-stream Mach numbers of 3 and (2) a reduction of centerline offset from inlet to diffuser exit. The inlet was investigated as a nose inlet (thus assuming complete external boundary-layer removal) at zero angle of attack and yaw.

Preliminary tests indicated the need for roughness on the spike tip. Without roughness the cone boundary layer bridged the juncture between first- and second-cone compression surfaces, resulting in an additional weak shock on the first cone and mislocation of the second strong shock. In order to have a shock configuration more likely to be encountered in flight, a 1/8-inch-wide strip of No. 100 carborundum dust was added near the tip of the first cone. The cone boundary layer then remained attached and the compression shocks met at the inlet lip, approximating closely the design conditions. This roughness was used for all tests.

Schematic drawings of the models investigated are presented in figure 1. Two basic configurations were used and will be designated herein as the short and long diffuser models. With the short diffuser model, expansion to the final diffuser area was completed at model station 14.28. The remaining model length (to station 21.97) was allotted for a constant-area mixing section, equivalent in length to 3.5 diffuser-exit diameters. For the long diffuser, expansion was not completed until station 18.68. The remaining model length (1.5 exit diameters) was again used as a constant-area mixing section. Stations within the constant-area mixing sections for both models will be given in terms of the constant-area mixing-length parameter L/D, where D is the diameter of the section.

With the short diffuser model, two internal centerbody fairings were investigated, as indicated in figure 1(a). For the majority of

these tests, the centerbody fairing was located along the floor of the model. For a limited number of tests, however, the centerbody fairing was raised off the inlet floor into the diffuser duct passage.

The effects of two additional modifications to the short diffuser model were also investigated, namely (1) the effect of a rapid acceleration of the flow at the diffuser exit and (2) the effect of internal bleed in the region of the inlet throat. These modifications to the basic diffuser are illustrated in figure 2.

As indicated in figure 2(a), acceleration of the flow was achieved by the insertion of a wooden contraction section at the diffuser exit. Contraction of the diffuser-exit diameter from 2.2 to 1.8 inches was achieved by an arbitrary fairing between model stations 14.28 and 15.28. A constant-area mixing section was maintained between model stations 15.28 and 18.28.

Internal bleed was achieved by bleeding air with four rows of holes through the inlet splitter plate between the centerbody and the inlet cowl (fig. 2(b)). The total area of the bleed holes was 0.092 square inch.

The constant-area mixing sections were enclosed with interchangeable sleeves upon which screens of various blockage area or solidity were mounted. Thus, the screen solidity and screen location was readily varied. Screens were located in the constant-area mixing section and also in the divergent part of the diffuser. A photograph of the screens which were mounted in the constant-area mixing section is presented in figure 3. When the screens were located in the diverging part of the diffuser, the screens were contoured to fit the internal flow passage.

Three combinations of screen mesh and wire diameter resulting in approximately 23-percent solidity were investigated for one configuration. However, unless otherwise noted, the 23-percent-solidity screen utilized for the majority of the tests had a wire mesh of 2 and a wire diameter of 0.062 inch.

Subsonic-diffuser area variations for the two basic models are given in figure 4. The initial diffuser-area expansion was determined by using the criterion of constant proportionality between the static-pressure gradient and the local static pressure (ref. 6). The area distribution for the remaining diffuser length was an arbitrary fairing which reduced the expansion rate at the downstream end of the diffuser. The area distribution for the raised centerbody model was not changed from that of the basic short diffuser model.

Instrumentation. - Two total-pressure rakes were utilized as shown in figure 1. The primary rake, which was longitudinally positioned by remote control, was used to determine the total-pressure distortion and total-pressure recovery at any station L within the constant-area mixing section. The secondary rake was used in the calculation of inlet mass flow, with the assumption of a choked exit plug. Locations of the tubes in the primary rake are given in figure 5. With the exception of the center tube, each of the 25 total-pressure tubes was located at the centroid of equal areas. When the contracting section was installed, the outermost tube of each rake segment was removed and the constant-area-section radius was reduced to that indicated by the dashed line. The remaining tubes were again located at the centroids of equal areas. The secondary rake was similarly constructed but was composed of 40 tubes.

Additional instrumentation included static-pressure taps located in the inlet cowl throughout the throat region and in the constant-area mixing section. The cowl-lip static-pressure taps were used to aid in positioning the inlet terminal shock, whereas the static-pressure taps in the mixing section were used to determine the pressure loss across the screens.

A total-pressure rake was also installed in the inlet throat at station 0 at the beginning of the investigation. This instrumentation, however, was removed for the remainder of the tests.

DISCUSSION OF RESULTS

Any numerical definition of flow distortion is incomplete by itself, since the effects of distortions entering the compressor (or the ram-jet combustion chamber) depend not only on the percentage distortion but also upon the distributions of the flow distortion. Thus, radial and circumferential distortions may have entirely different effects upon compressor surge and stall characteristics. Hence, total-pressure or velocity contours are needed to completely define flow distortion.

However, for the purposes of this report a definition of distortion by which the severity of a distorted flow is represented by a single number is useful, since it provides a convenient basis for comparison of the methods of distortion reduction investigated. Other specific considerations of the resultant distortions can be obtained from the reported total-pressure contours. Flow distortion, as discussed herein, is defined as the maximum total-pressure variation obtained from the pitot tubes of the primary rake divided by the average total pressure, or

$$\text{Percent flow distortion} = \frac{\Delta P}{P_{av}} \times 100 = \left(\frac{P_{l,max} - P_{l,min}}{P_{av}} \right) \times 100$$

Distortion at inlet throat. - During the initial phase of the investigation, the flow in the inlet throat was surveyed with total-pressure rakes, and the results are presented in figure 6 for the maximum-pressure-recovery condition. Large total-pressure distortions were observed, as evidenced by the low pressures in the corners of the inlet and the relatively high pressures at the top of the inlet. The low-pressure region is caused by an accumulation of the compression-surface boundary layer. Presented for comparison is the theoretical shock pressure recovery based on flow through the two oblique compression shocks and the inlet terminal shock. Pressure recoveries measured across the top of the inlet were higher than this theoretical value, presumably because of the presence of additional weak shocks caused by shock - boundary-layer interaction which were not accounted for by the theoretical value.

Effect of inlet operating conditions. - The majority of the test data were obtained with the short diffuser model. The pressure recovery and the mass-flow performance of this model are presented in figure 7 for several longitudinal locations of the primary rake in the constant-area mixing section. Small changes in subcritical inlet operation were noted as the primary rake was moved rearward in the constant-area mixing section. These changes may have been due to the pressure-weighting technique used, although the cowl-lip static-pressure taps indicated that a branched or lambda form of the normal shock moved farther forward into the inlet throat as the primary rake was moved downstream. In any case, the variations in the data are probably within the experimental accuracy, and it is clear that little or no loss in pressure recovery occurred through use of the constant-area mixing sections. The supercritical inlet mass-flow ratio was 0.996, while the average maximum pressure recovery was about 62 percent of the free-stream value. The average maximum pressure for this and other configurations investigated is summarized in table 1.

Total-pressure contours obtained at rake station 14.28 (L/D = 0) are presented in figure 8 for several values of the average Mach number ahead of the rake. The lines labeled $\left(\frac{P_l}{P_{av}} - 1\right)$ indicate isobars of total pressures expressed in percent above or below the average pressure recovery. For example, for a rake Mach number of 0.197, a high-pressure core 10.2 percent larger than the average pressure recovery (0.615) was measured. Likewise, total pressures 6 percent below the average pressure were measured with the rake tubes closest to the diffuser wall. Thus, the total distortion was about 16.2 percent.

The cores of high-pressure air indicate incomplete mixing of the distortion which existed in the inlet throat (fig. 6). Changes in inlet operation (i.e., rake Mach number) did not change appreciably the location of these cores in the duct passage.

The effect of mode of inlet operation on the total-pressure distortion at the diffuser exit is summarized in figure 9. Distortion and total-pressure-recovery data are given as a function of the rake Mach number. Operation of the inlet in the supercritical regime increased the distortion considerably over that obtained for critical inlet operation. Subcritical inlet operation reduced the distortion only slightly below that obtained at critical inlet operation. The total-pressure plot at the top of the figure indicates that the minimum distortion occurred at the maximum-pressure-recovery condition.

Effect of constant-area mixing sections on flow distortion. - The effect of increasing the effective model length by the addition of constant-area mixing sections at the end of the diffuser is presented in figure 10. For all inlet operating conditions the total-pressure distortion decreased when the length of the constant-area mixing section was increased. The addition of mixing length, however, was most effective when the entering distortion level was high. This results from increased mixing due to the higher shear of the badly distorted profile. The distortion level was lowest for inlet operation at the maximum-pressure-recovery condition for all values of L/D. The distortion data for the remainder of this report were obtained at the maximum-pressure-recovery condition.

Effect of diffuser length. - A limited number of tests were run with the long diffuser model. Distortion data for this model are presented as a function of model station in figure 11 and compared with corresponding data for the short diffuser model. At the beginning of the constant-area mixing section the long diffuser yielded the lower distortion, presumably because of the longer mixing length of the long diffuser model. However, the addition of constant-area mixing length to the short diffuser rapidly reduced its distortion so that for a comparable over-all model length a lower distortion was obtained with the short diffuser. The increased mixing obtained with the short diffuser model plus constant-area section is probably due to the lower average Mach number and hence increased shear of the short diffuser model. A somewhat lower pressure recovery was obtained with the long diffuser model. Additional investigation is needed to determine the optimum combination of diffuser plus constant-area length to arrive at a minimum distortion without incurring an excessive total-pressure loss.

Effect of screens. - Several combinations of screen solidity, mesh, and location in the duct passage were investigated with the short diffuser model. Only limited screen data, however, were obtained with the long diffuser model.

Inlet performance data of the short diffuser model with several screens located at model station 14.28 are presented in figure 12.

As was previously mentioned, small changes in subcritical inlet operation were noted as the position on the primary rake was changed. The average performance data of figure 7 for the model without internal screen have been added to the screen data of figure 12 for purposes of comparison. The addition of internal screens increased the subcritical stability but decreased the maximum pressure recoveries by less than 1 percent for the 10- and 23-percent-solidity screens and by about 2 percent for the 40-percent-solidity screen.

Total-pressure contours for the screen configurations are presented in figure 13 for the maximum-pressure-recovery condition. A comparison of the profiles measured at L/D of 0.46 with those obtained without screens (fig. 8) indicates that the high-pressure core did not move from its location in the upper part of the duct as the air passed through the screens. However, the total-pressure distortion was reduced considerably. The movement of the survey rake farther downstream into the constant-area section indicated further reductions in distortion and showed a tendency for the high-pressure core to move to the lower part of the duct.

The effect of screens on total-pressure distortion is summarized in figures 14(a) and (b) for the short and long diffuser models, respectively. The effective reduction of distortion by the addition of screen blockage and mixing length is quite evident. The data of figure 14(a) show that without screen blockage a constant-area mixing length of about 3.2 diffuser-exit diameters would be required to reduce the distortion to 5 percent. By using a screen of 40-percent solidity, the necessary mixing length could be reduced to 0.6 diameter. Each of these two configurations suffer penalties in order to attain the 5-percent distortion level. In the case of the screen, a pressure loss is encountered and operational problems such as icing will occur. For the constant-area mixing-length configuration, added weight and volume are required.

The effects of varying the screen mesh and diameter while maintaining a solidity of about 23 percent are given in figure 15. The effect of screen mesh was not negligible inasmuch as the over-all change in distortion was about as much as was found in figure 14(a) for a change in solidity from 10 to 23 percent. However, the maximum pressure recovery was not changed appreciably for the change in screen mesh. Additional study on the effects of screen mesh is required.

In order to determine the effect of screen location on distortion, screens were also located in the expanding section of the diffuser at station 11 and downstream of the beginning of the constant-area mixing section at station 16.28 in the short diffuser model. The results of this comparison are presented in figure 16. When the screens were located at these stations rather than at the end of the diffuser, somewhat larger distortions were measured.

Total-pressure losses across the screens for the short diffuser model are summarized and compared with predicted losses from reference 7 in figure 17. Total-pressure loss is plotted as a function of screen solidity for average flow Mach numbers ahead of the screen of 0.20 and 0.34. These Mach numbers correspond to those ahead of the screen at the maximum-pressure-recovery condition for screens located at model stations 14.28 and 11.00, respectively.

When the screens were installed at station 14.28, the total-pressure losses were somewhat larger than had been predicted. These losses, which were determined by taking the difference between measured rake total pressures with and without screens, agreed with the losses determined from the measured static-pressure rise across the screens.

In a similar test of screens for a wing-root inlet (ref. 2), the agreement between actual and predicted losses was not so good as that obtained herein. Apparently, inasmuch as the data of reference 7 were obtained with nearly uniform flow approaching the screens, the better agreement of the present data is probably due to a more uniform profile approaching the screen than was the case with reference 2.

When the screens were installed in the expanding section of the diffuser, the measured screen losses were expected to increase as a result of the increase in approach Mach number. However, as indicated in figure 17, increased losses were observed only for the 40-percent-solidity screen and even this loss was lower than had been predicted. The anticipated losses due to the higher flow Mach number appeared to have been offset by more optimum supersonic compression as evidenced by the cowl-lip static-pressure taps. This result may have been due to differences in spike tip roughness between configurations.

It should be noted that for lower free-stream Mach numbers, the diffuser-exit Mach number would be higher than that obtained with the present model in order to satisfy the weight-flow requirements of a turbojet engine. With these higher duct Mach numbers, the losses across the screens would be larger than were measured herein.

Effect of acceleration at diffuser exit. - In addition to constant-area mixing length and forced mixing devices, other methods have been proposed as possible means of reducing flow distortion. One of these methods consists of the use of a rapid acceleration of the flow at the diffuser exit (ref. 4). To determine the effect of such an acceleration, a wooden contraction section was fitted into the sleeve section at the end of the diffuser (fig. 2(a)).

The performance curves of the contracted diffuser configuration are presented in figure 18. Total-pressure profiles for maximum-pressure-recovery operation are presented in figure 19 for several

constant-area mixing lengths, and the distortion data are summarized in figure 20. An appreciable reduction in distortion was achieved with no loss of pressure recovery.

Effect of change in flow passage shape. - Another method of distortion reduction is associated with shock - boundary-layer interaction and distortions arising from local separations within the diffuser. An example of this approach was used in reference 8, where it was found that the addition of fillets in the corners of a side inlet reduced the distortion. In the present investigation the effect of a simple change in internal geometry obtained by raising the internal centerbody fairing from the duct floor into the duct passage (fig. 1) was determined.

Total-pressure contours are presented in figure 21 for several values of L/D. Contours at increasing values of L/D indicate a clockwise rotation of the high-pressure core, suggesting that the centerbody may not have been alined with the model axis.

Distortion data for the raised centerbody model are summarized and compared with the original model in figure 22. A considerable reduction in distortion was achieved by raising the centerbody, although a total-pressure loss of 0.04 was incurred. This loss might have been reduced by redesigning the centerbody fairing so that its tip was more nearly at the centerline of the exit duct.

The installation of screens at station 14.28 reduced the distortion of the raised centerbody model to even lower values. These data are presented in figure 23. With the 40-percent-solidity screen installed, a minimum distortion of about 1.4 percent was obtained. However, additional pressure losses were incurred with the screen configurations.

Effect of internal throat bleed. - Pressure instrumentation at the inlet throat indicated the presence of boundary layer in the corners of the inlet (fig. 6). Removal of this boundary layer would reduce the distortion entering the diffuser and therefore should reduce the distortion at the exit of the diffuser. Boundary-layer removal was therefore provided by bleeding at the inlet throat (fig. 2(b)).

Inlet performance with this internal bleed is presented in figure 24. During supercritical inlet operation a spillage of about 2 percent mass flow occurred. When the internal normal shock moved into the region of the bleed holes, the amount of bleed increased to about 8 percent. The maximum pressure recovery (64 percent) was obtained with this configuration.

The distortion data of the bleed configuration are compared with the original configuration in figure 25 for the maximum-pressure-recovery condition. Internal bleed effectively reduced the distortion and also increased the maximum pressure recovery.

General remarks. - It has been demonstrated that distorted total-pressure profiles can be improved by mixing. This mixing can either be obtained by allowing sufficient passage length or, if length is not available, mixing can be forced by screens. Each method, however, is not without penalty. Excessively long ducts require additional weight and volume. The use of screens incurs penalties in the form of pressure losses and introduces operating problems.

Apparently, the best way to reduce distortion would be to reduce it at its source, that is, near the inlet throat. It was demonstrated that bleeding from the throat section reduced distortion and at the same time improved the over-all pressure recovery. The effects of flow passage shapes and local surface curvatures may be equally important.

If excessive distortion still exists and if space is available, the distortion could possibly be reduced by overexpanding the diffuser to a low Mach number. The use of a screen followed by a rapid acceleration of the flow should then permit low flow distortions with little loss in pressure recovery.

SUMMARY OF RESULTS

Several methods of straightening diffuser-exit total-pressure profiles were investigated using a typical side-inlet model at a Mach number of 3.05. The methods studied include (a) longer subsonic diffusers, (b) constant-area mixing sections, (c) internal screens, (d) a contraction section, (e) internal bleed, and (f) a change in internal flow passage shape. The results of this investigation may be summarized as follows:

1. Increasing the diffuser length was found to be quite effective in reducing the total-pressure distortion. Thus, increasing the effective model length by the addition of constant-area mixing sections at the end of the diffuser was found to be effective with little or no loss in pressure recovery. Also, increasing the basic diffuser length was effective, and the longer of two subsonic diffuser models yielded lower distortions at the end of the diffusing section.

2. The use of screens as forced mixing devices effectively reduced distortion at the expense of a loss in pressure recovery.

3. The use of either a contraction section at the end of the diffuser or internal bleed from the inlet throat region reduced the distortion with no loss in pressure recovery.

4. Raising the centerbody fairing from the inlet floor into the diffuser duct reduced the distortion effectively; however, the reduction was obtained at the expense of a pressure-recovery loss.

Lewis Flight Propulsion Laboratory
National Advisory Committee for Aeronautics
Cleveland, Ohio, June 24, 1955

REFERENCES

1. Wallner, Lewis E., Conrad, E. William, and Prince, William R.: Effect of Uneven Air-Flow Distribution to the Twin Inlets of an Axial-Flow Turbojet Engine. NACA RM E52K06, 1953.

2. Piercy, Thomas G., and Weinstein, Maynard I.: Preliminary Investigation at Mach Number 1.9 of Simulated Wing-Root Inlets. NACA RM E54I24, 1955.

3. Farley, John M., and Seashore, Ferris L.: Full-Scale, Free-Jet Investigation of Methods of Improving Outlet Flow Distribution in a Side-Inlet Supersonic Diffuser. NACA RM E54L31a, 1955.

4. Johnston, I. H.: The Use of Freely Rotating Blade Rows to Improve Velocity Distributions in an Annulus. Memo. No. M.109, British N.G.T.E., 1951.

5. Johnson, Harry W., and Piercy, Thomas G.: Effect of Wedge-Type Boundary-Layer Diverters on Performance of Half-Conical Side Inlets at Mach Number 2.96. NACA RM E54E20, 1954.

6. Davis, Wallace F., Edwards, Sherman S., and Brajnikoff, George B.: Experimental Investigations at Supersonic Speeds of Twin-Scoop Duct Inlets of Equal Area. IV - Some Effects of Internal Duct Shape Upon an Inlet Enclosing 37.2 Percent of the Forebody Circumference. NACA RM A9A31, 1949.

7. Adler, Alfred A.: Variation with Mach Number of Static and Total Pressures Through Various Screens. NACA WR L-23, 1946. (Supersedes NACA CB L5F28.)

8. Valerino, Alfred S.: Effects of Internal Corner Fillets on Pressure Recovery - Mass Flow Characteristics of Scoop-Type Conical Supersonic Inlets. NACA RM E52J10, 1952.

TABLE I. - SUMMARY OF MAXIMUM-PRESSURE-RECOVERY DATA FOR ALL CONFIGURATIONS

Basic diffuser	Alteration to basic model	Screen location, model station	Screen mesh (number of wires per in.)	Wire diameter, in.	Average maximum total-pressure recovery
Short diffuser	----------	-----	---	-----	0.620
	10-Percent-solidity screen	14.28	5	0.010	.616
	23-Percent-solidity screen	14.28	2	.062	.611
	40-Percent-solidity screen	14.28	7	.031	.599
	23-Percent-solidity screen	14.28	4	.031	.613
	25-Percent-solidity screen	14.28	2.7	.051	.611
	10-Percent-solidity screen	16.28	5	.010	.618
	23-Percent-solidity screen	16.28	2	.062	.614
	40-Percent-solidity screen	16.28	7	.031	.605
	10-Percent-solidity screen	11.00	5	.010	.619
	23-Percent-solidity screen	11.00	2	.062	.616
	40-Percent-solidity screen	11.00	7	.031	.581
	Contraction section	-----	---	-----	.629
	Internal bleed	-----	---	-----	.635
Long diffuser	----------	-----	---	-----	0.600
	10-Percent-solidity screen	14.85	5	0.010	.594
	23-Percent-solidity screen	14.85	2	.062	.592
	40-Percent-solidity screen	14.85	7	.031	.564
Short diffuser with raised centerbody	----------	-----	---	-----	0.579
	10-Percent-solidity screen	14.28	5	0.010	.575
	23-Percent-solidity screen	14.28	2	.062	.572
	40-Percent-solidity screen	14.28	7	.031	.562

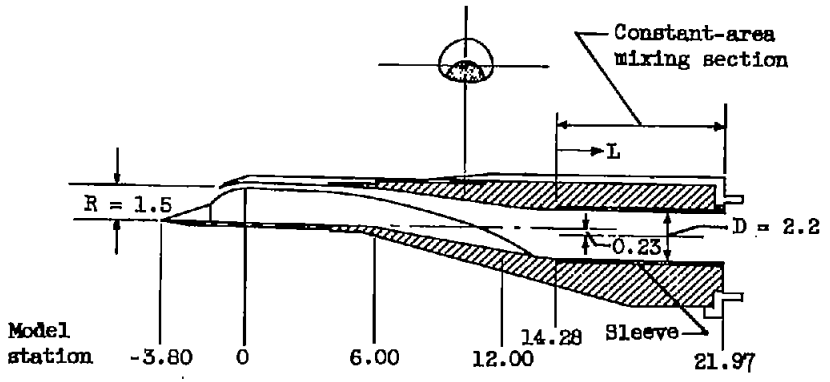

Centerbody on inlet floor

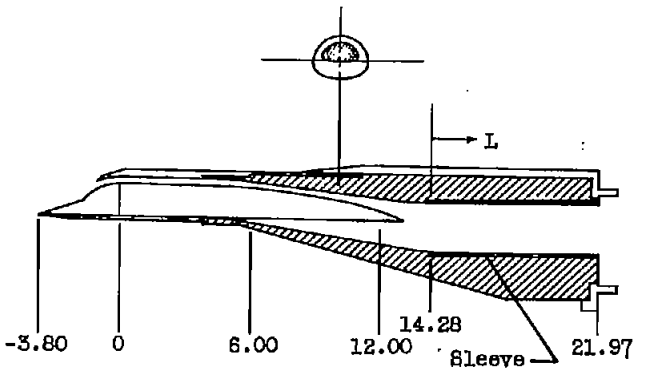

Raised centerbody fairing

(a) Short diffuser model.

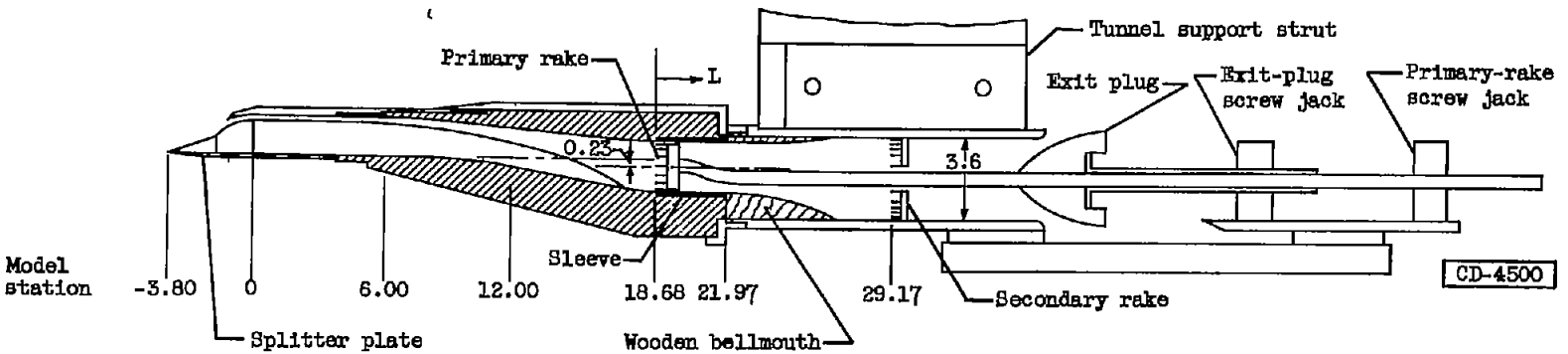

(b) Long diffuser model, with tunnel support apparatus.

Figure 1. - Schematic drawings of models. (All dimensions in inches.)

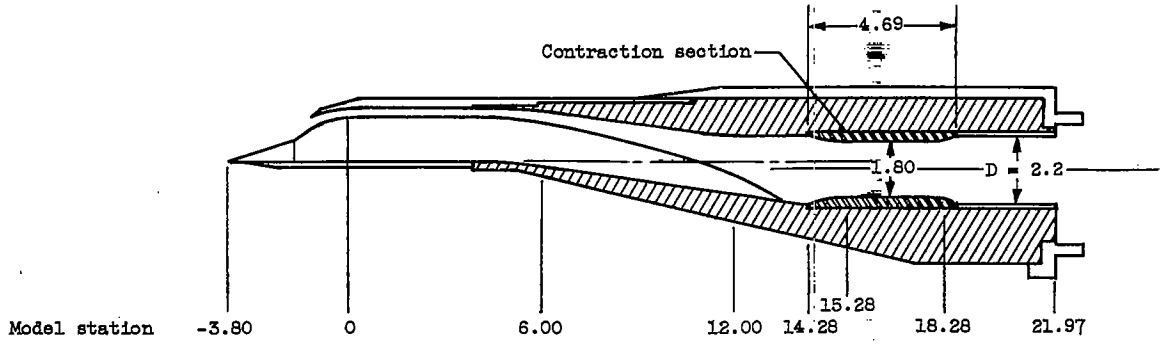

(a) Contraction section installed.

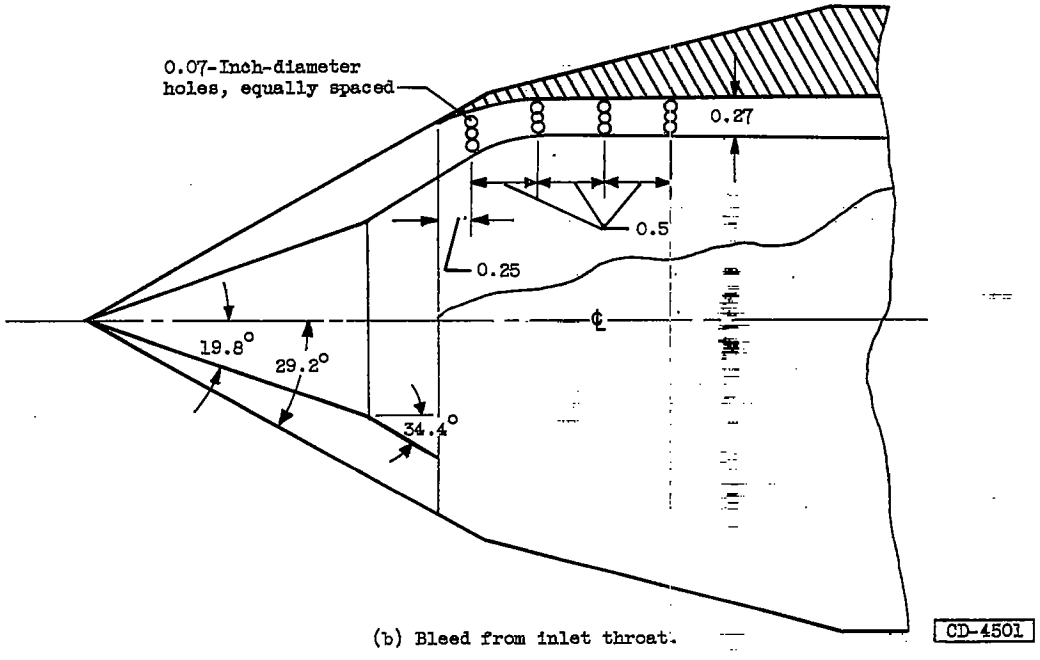

(b) Bleed from inlet throat. CD-4501

Figure 2. - Alterations to short diffuser model. (All dimensions in inches.)

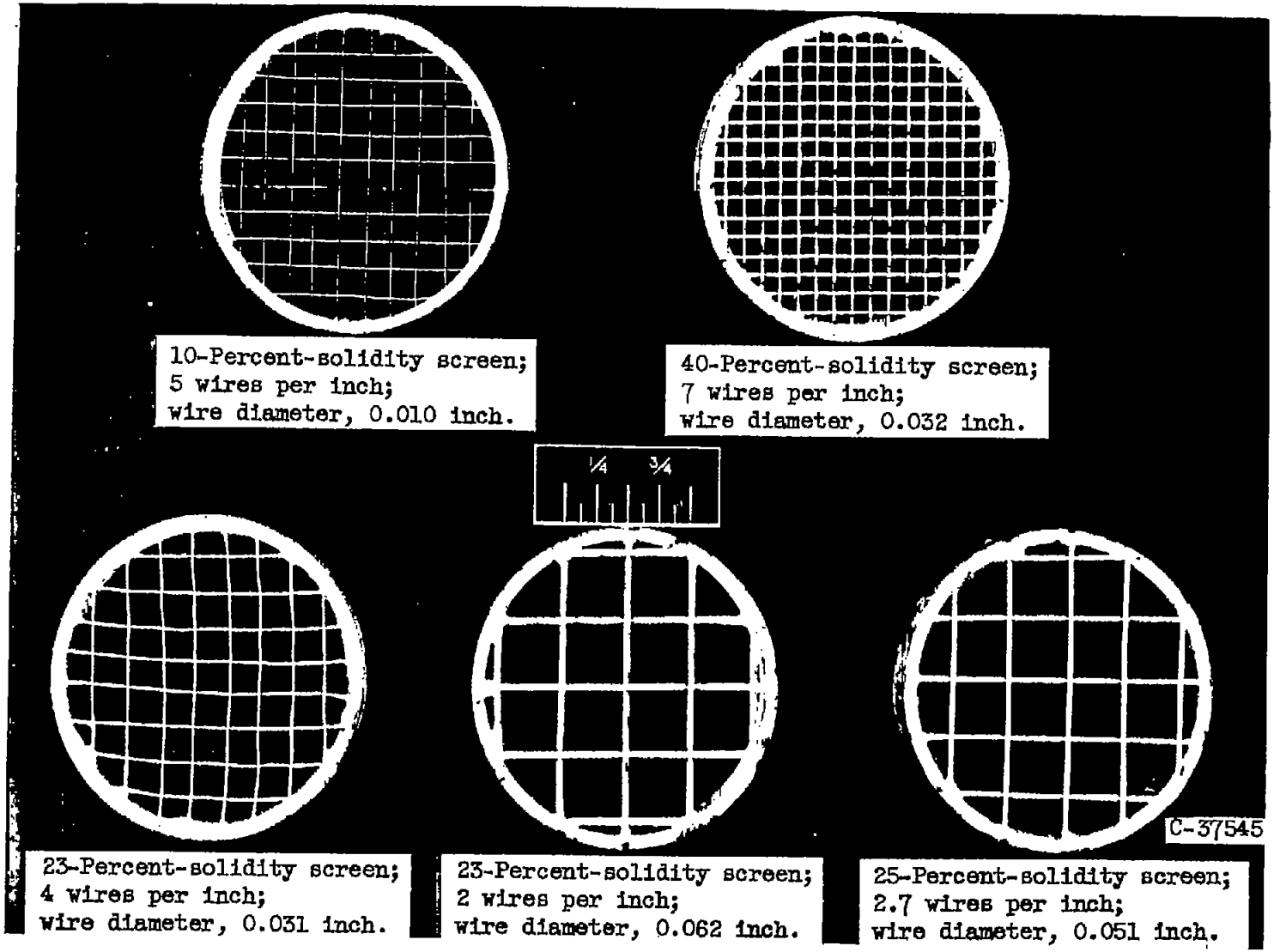

Figure 3. - Photograph of screens.

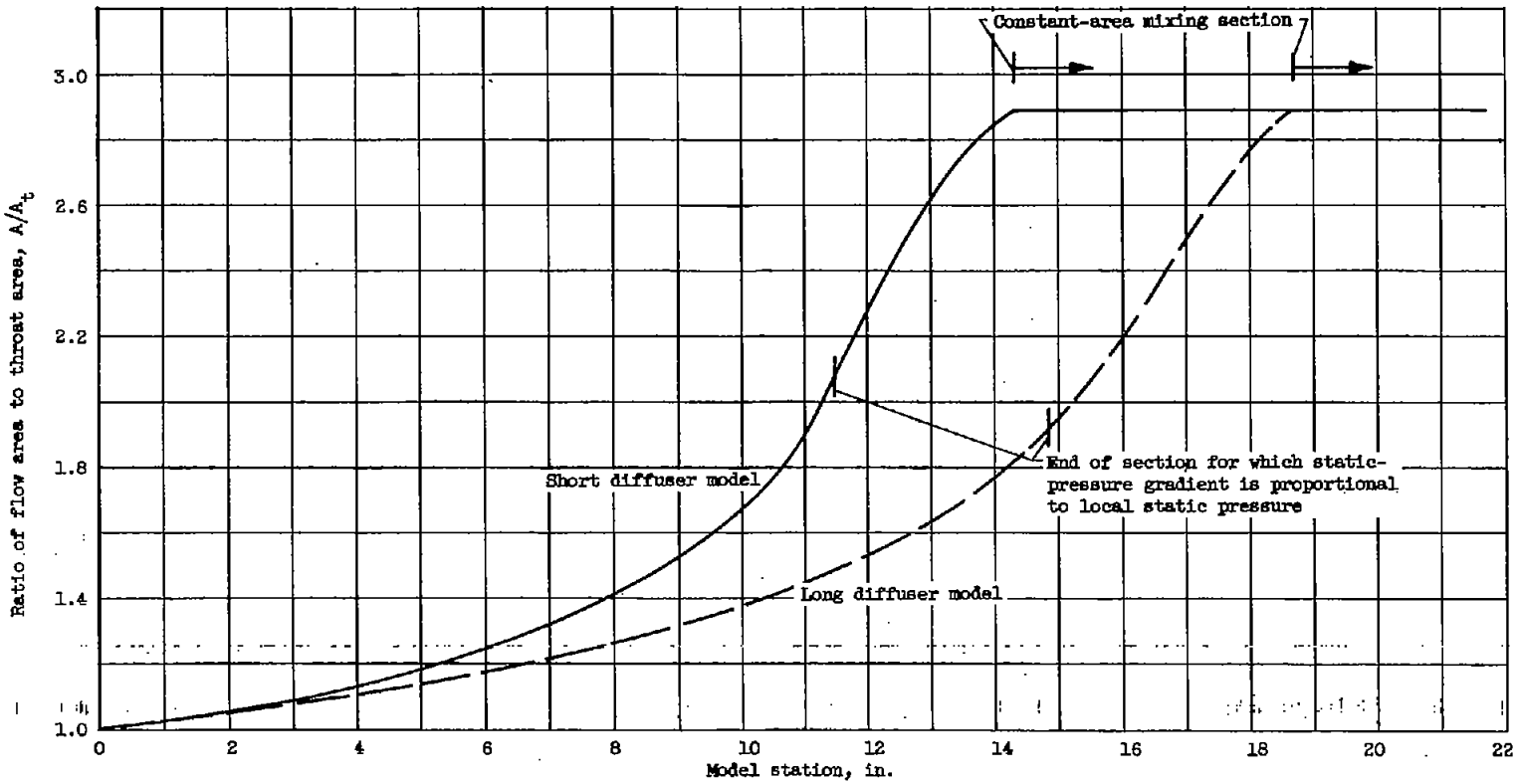

Figure 4. - Subsonic-diffuser area variations.

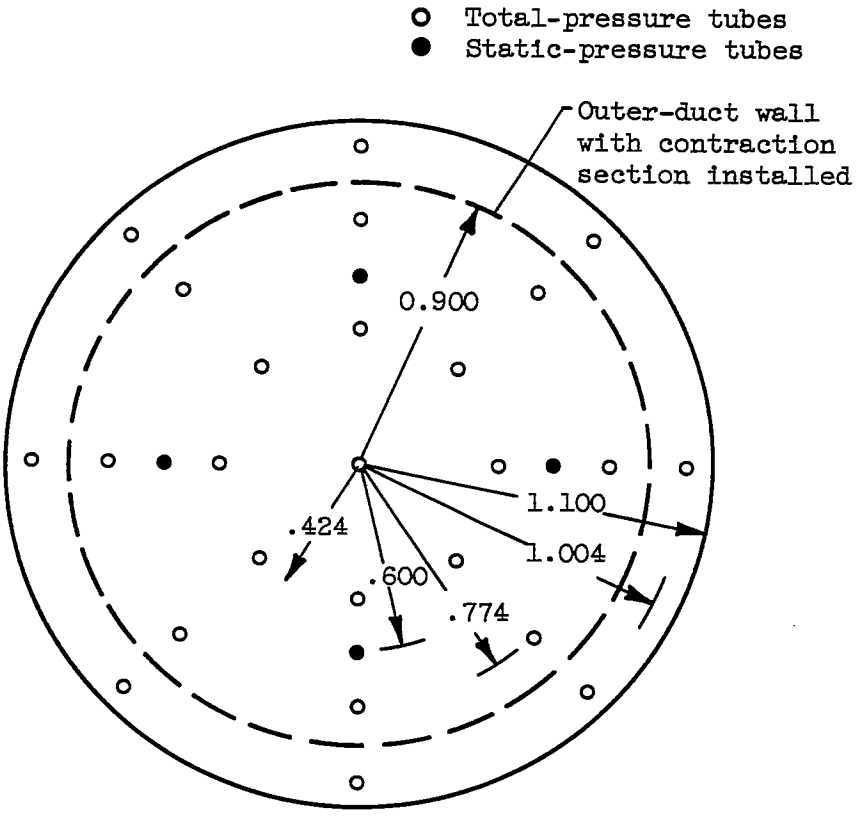

Figure 5. - Details of primary rake. (All dimensions are in inches.)

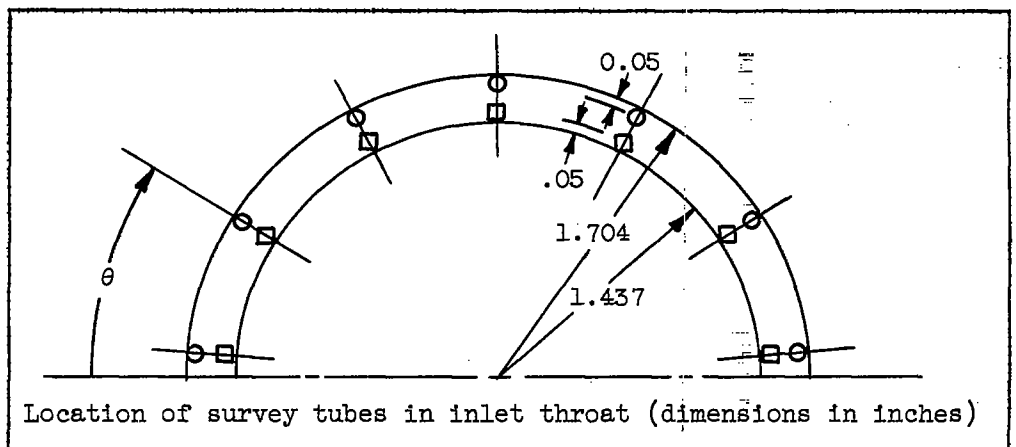

Location of survey tubes in inlet throat (dimensions in inches)

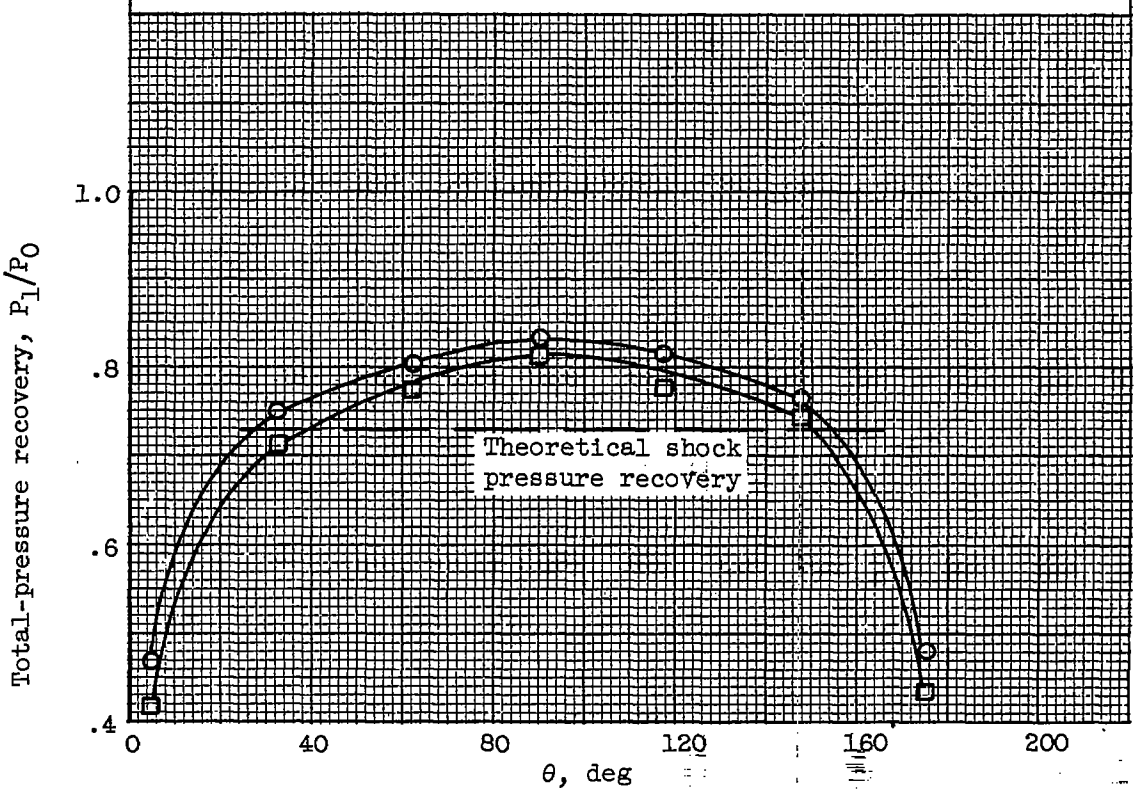

Figure 6. - Inlet-throat flow survey data.

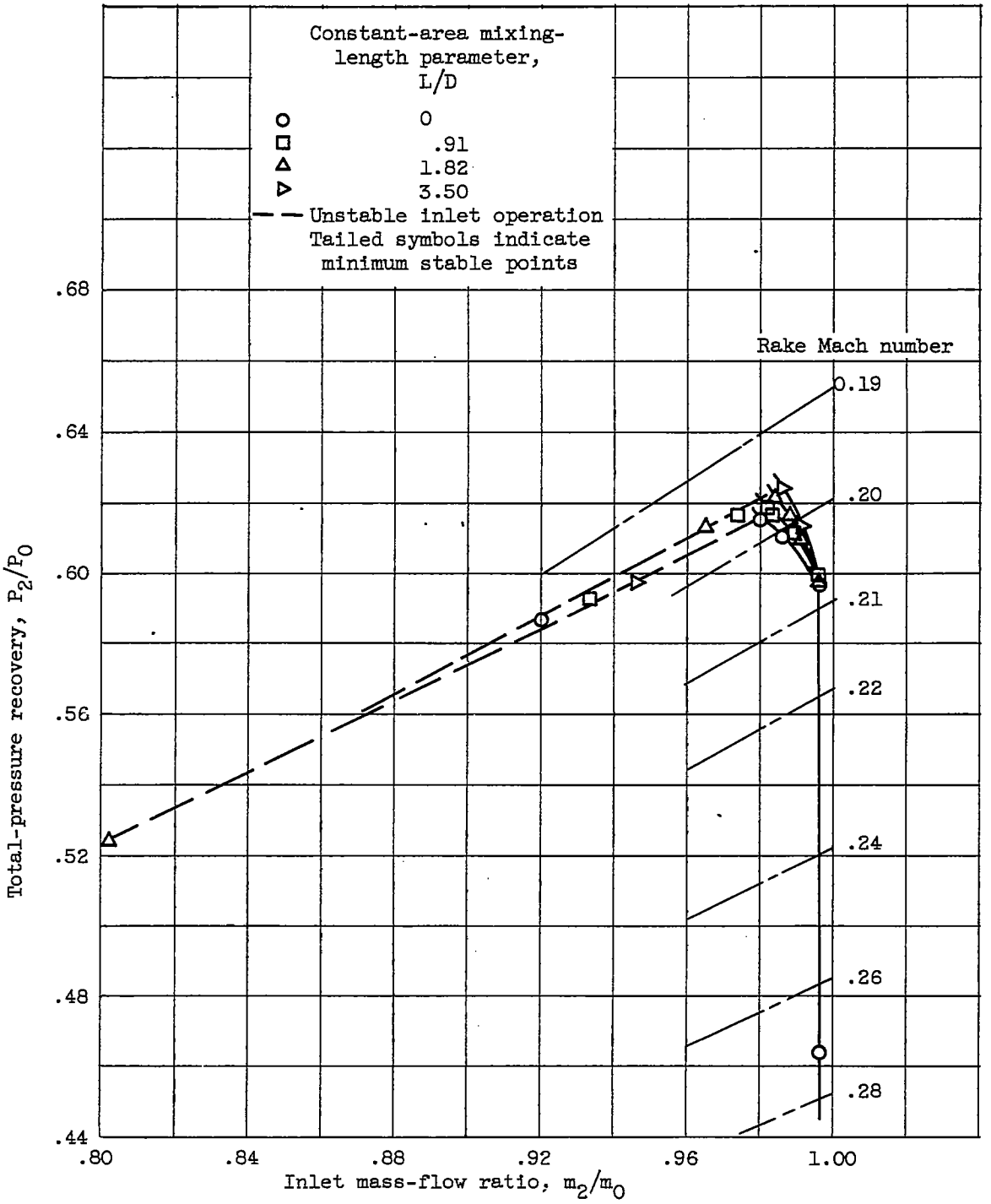

Figure 7. - Effect of constant-area mixing length on inlet performance. Short diffuser model.

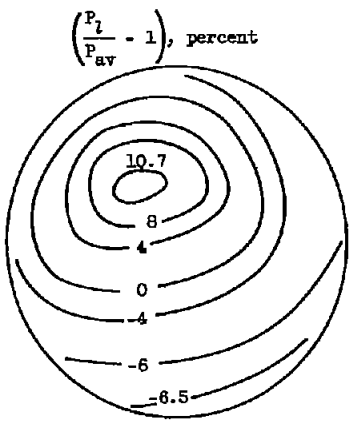

Rake Mach number, 0.195
Total-pressure distortion, $\Delta P/P_{av}$, 17.2 percent
Total-pressure recovery, P_{av}/P_0, 0.586
Inlet mass-flow ratio, m_2/m_0, 0.920

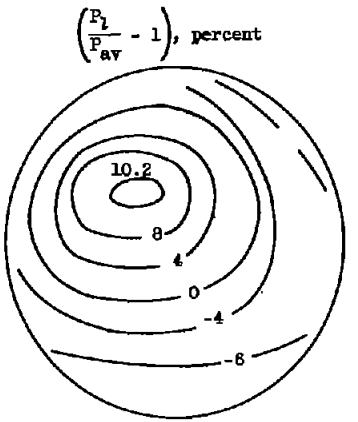

Rake Mach number, 0.197
$\Delta P/P_{av}$, 16.2 percent
P_{av}/P_0, 0.615
m_2/m_0, 0.980

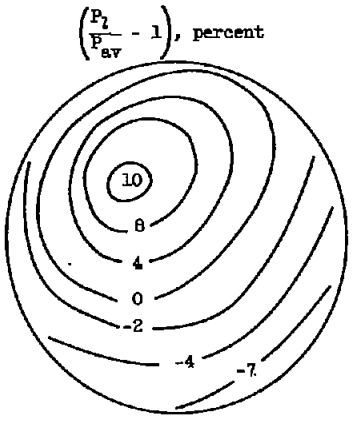

Rake Mach number, 0.201
$\Delta P/P_{av}$, 17.0 percent
P_{av}/P_0, 0.610
m_2/m_0, 0.986

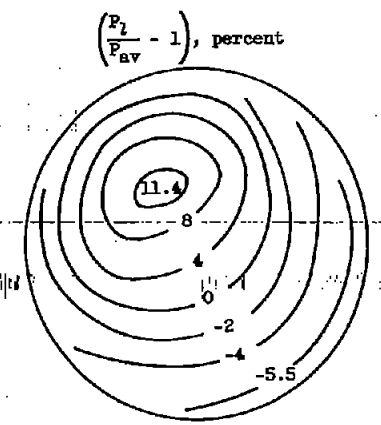

Rake Mach number, 0.208
$\Delta P/P_{av}$, 16.9 percent
P_{av}/P_0, 0.596
m_2/m_0, 0.996

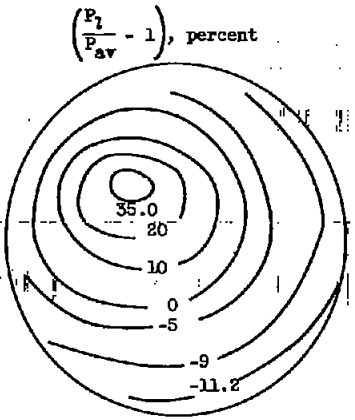

Rake Mach number, 0.275
$\Delta P/P_{av}$, 46.2 percent
P_{av}/P_0, 0.464
m_2/m_0, 0.996

Figure 8. - Total-pressure contours at primary rake. Short diffuser model; constant-area mixing-length parameter, 0.

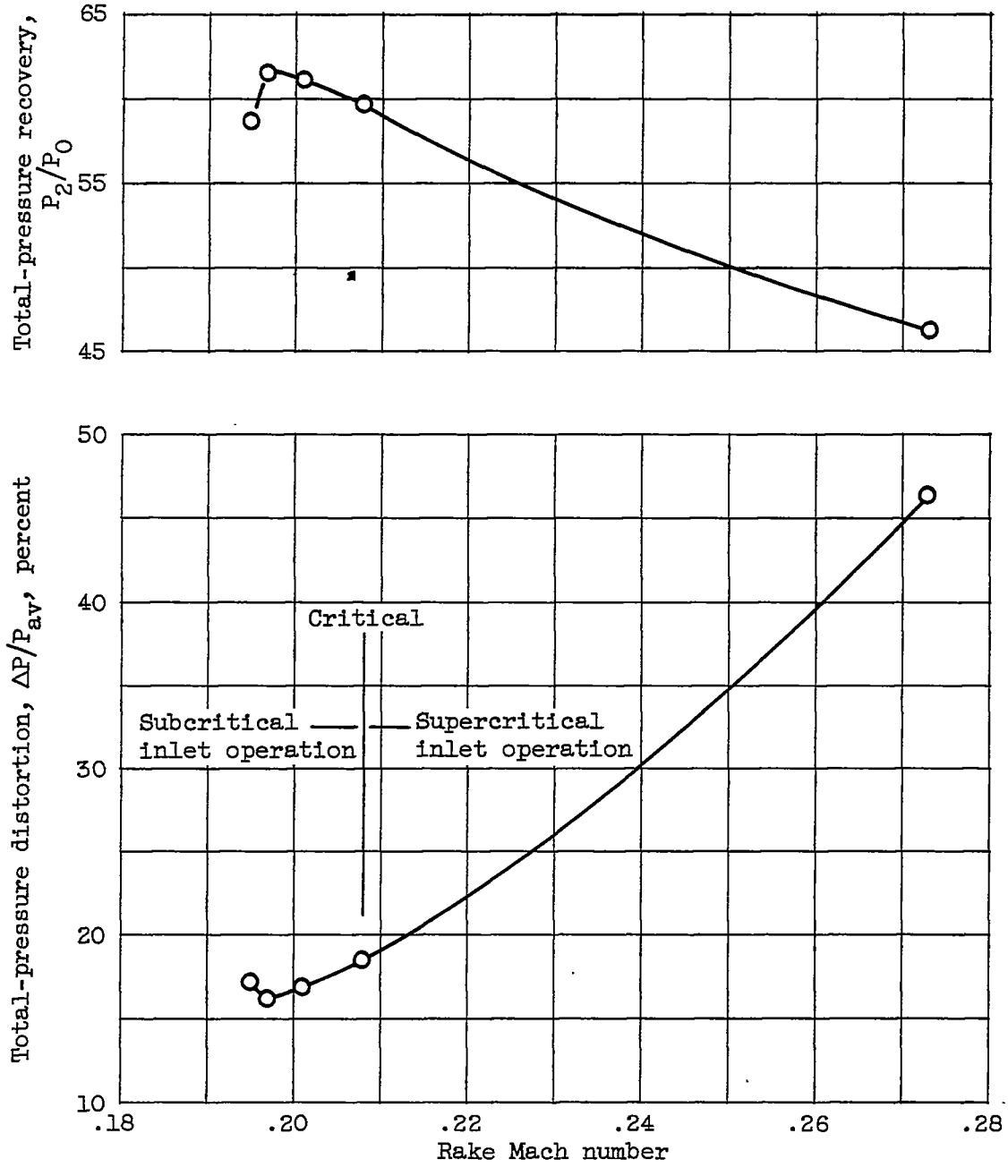

Figure 9. - Effect of inlet operation on total-pressure distortion. Short diffuser model; constant-area mixing-length parameter, 0.

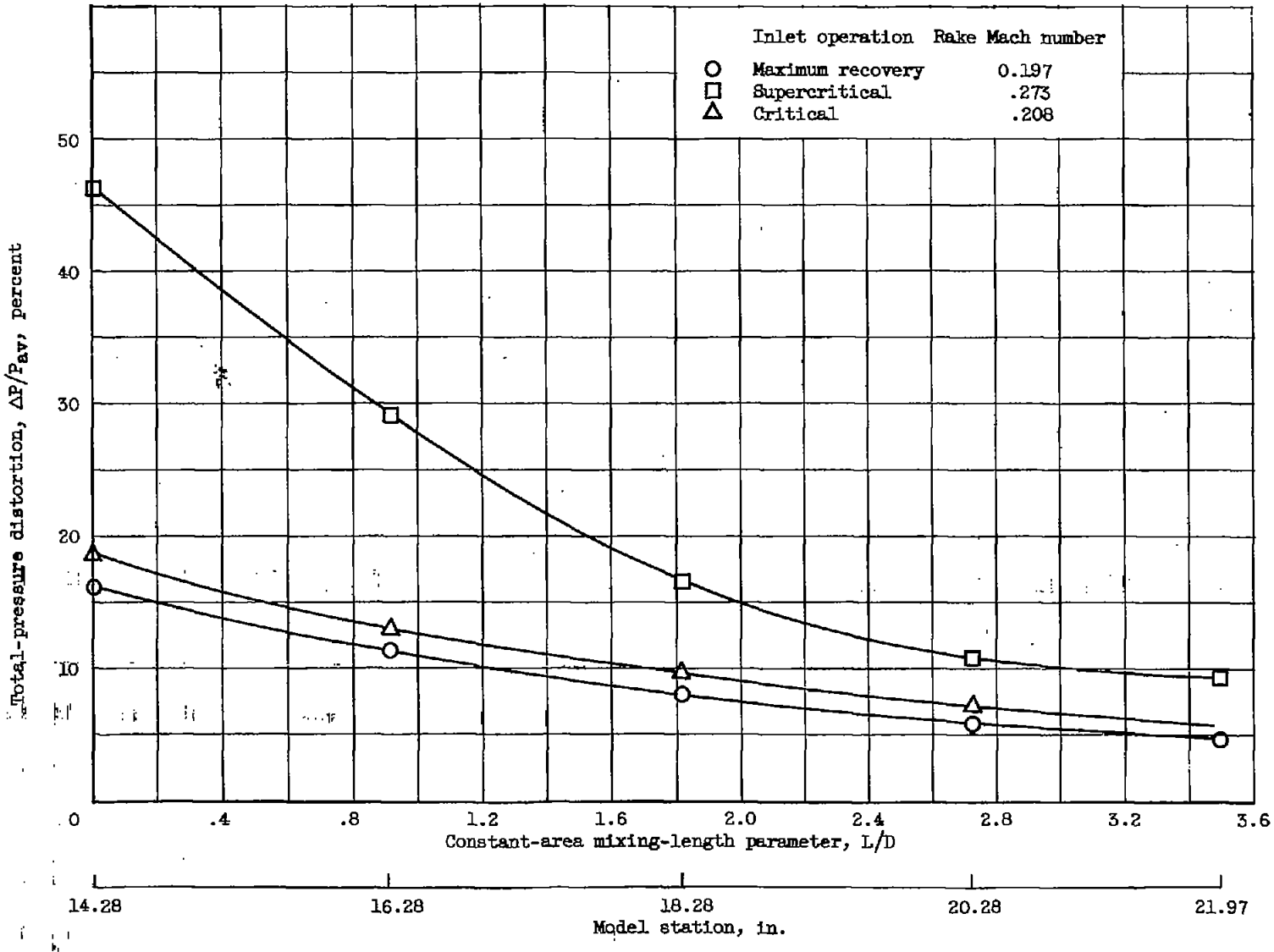

Figure 10. - Effect of constant-area mixing length on total-pressure distortion. Short diffuser model.

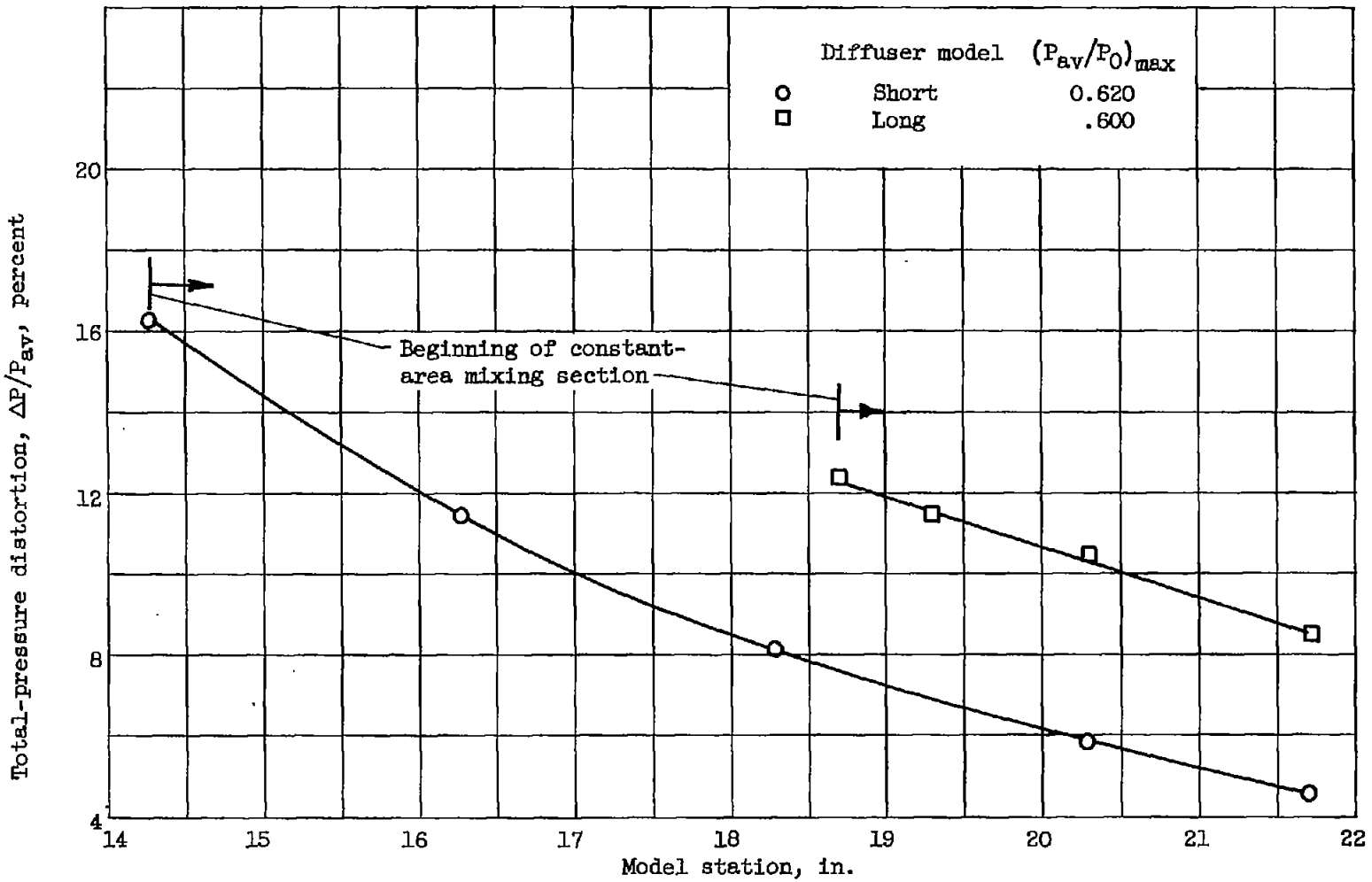

Figure 11. - Comparison of total-pressure distortion for two basic models.

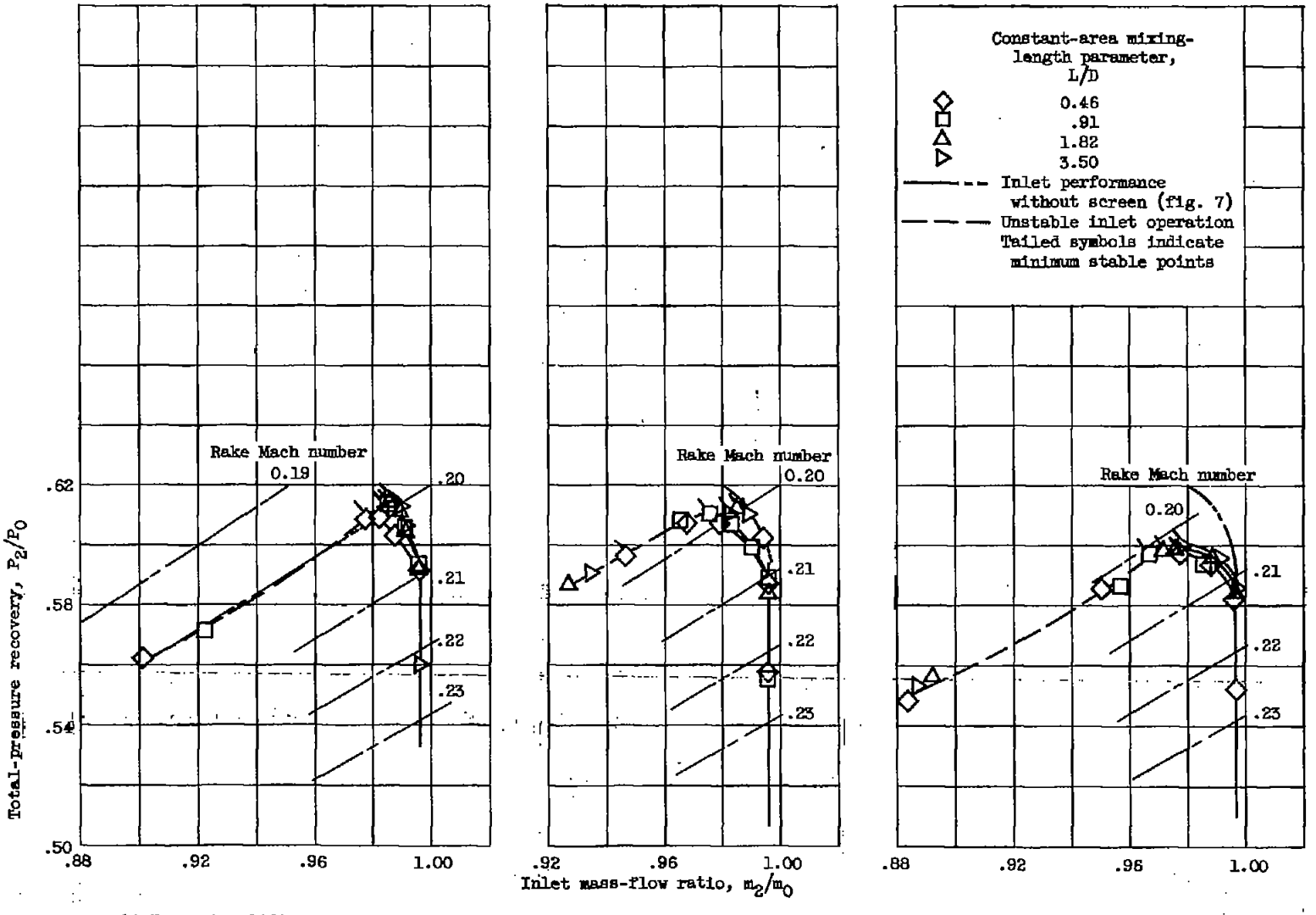

Figure 12. - Effect of internal screens on inlet performance. Short diffuser model; screens located at model station 14.28.

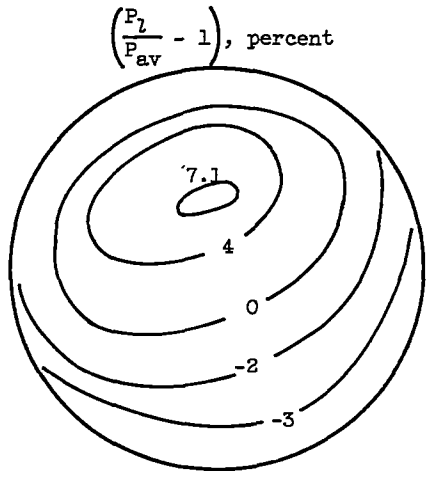

Constant-area mixing-length parameter, L/D, 0.46
Rake Mach number, 0.200
Total-pressure distortion, $\Delta P/P_{av}$, 10.4 percent
Total-pressure recovery, P_{av}/P_0, 0.609
Inlet mass-flow ratio, m_2/m_0, 0.982

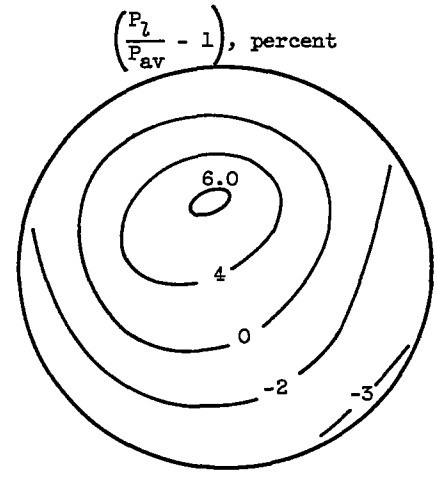

L/D, 0.91
Rake Mach number, 0.199
$\Delta P/P_{av}$, 9.0 percent
P_{av}/P_0, 0.614
m_2/m_0, 0.985

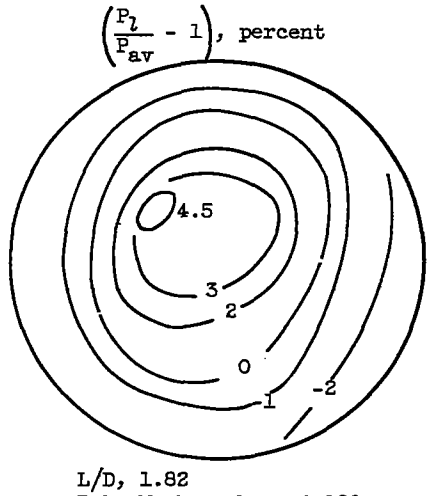

L/D, 1.82
Rake Mach number, 0.199
$\Delta P/P_{av}$, 6.8 percent
P_{av}/P_0, 0.615
m_2/m_0, 0.985

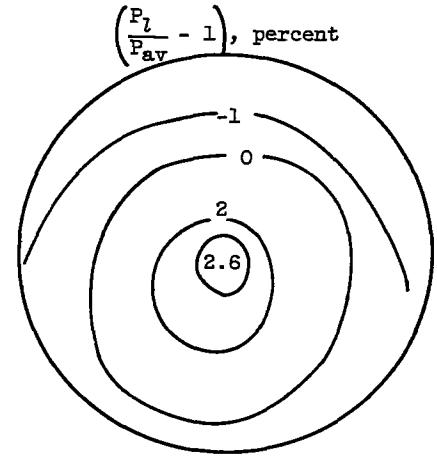

L/D, 3.50
Rake Mach number, 0.199
$\Delta P/P_{av}$, 4.0 percent
P_{av}/P_0, 0.616
m_2/m_0, 0.986

(a) 10-Percent-solidity screen.

Figure 13. - Effect of internal screens on total-pressure contours at primary rake. Short diffuser model; screens located at model station 14.28.

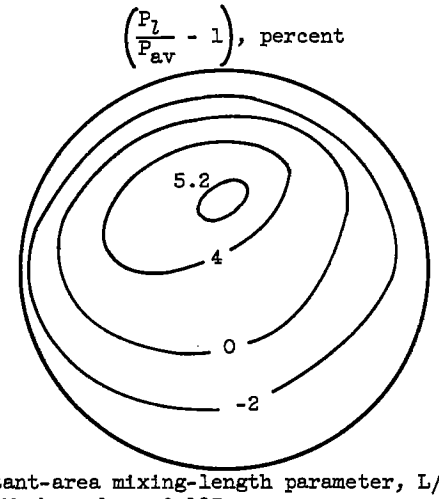

Constant-area mixing-length parameter, L/D, 0.46
Rake Mach number, 0.197
Total-pressure distortion, $\Delta P/P_{av}$, 7.3 percent
Total-pressure recovery, P_{av}/P_0, 0.608
Inlet mass-flow ratio, m_2/m_0, 0.967

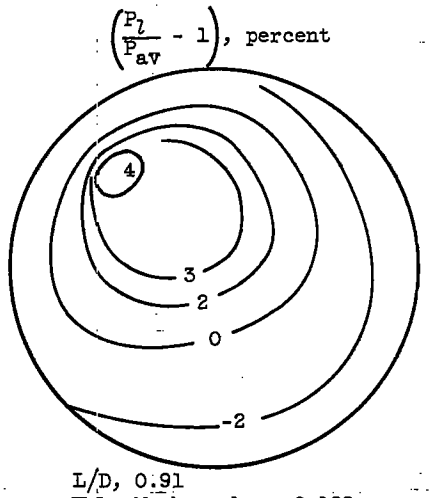

L/D, 0.91
Rake Mach number, 0.199
$\Delta P/P_{av}$, 6.4 percent
P_{av}/P_0, 0.610
m_2/m_0, 0.976

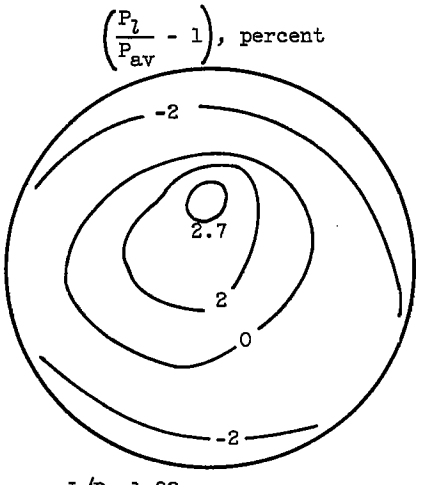

L/D, 1.82
Rake Mach number, 0.200
$\Delta P/P_{av}$, 5.2 percent
P_{av}/P_0, 0.613
m_2/m_0, 0.984

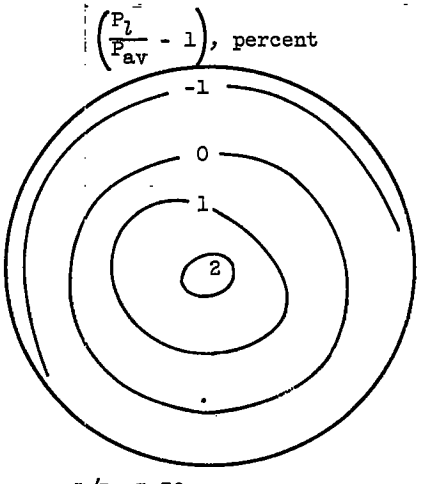

L/D, 3.50
Rake Mach number, 0.200
$\Delta P/P_{av}$, 3.4 percent
P_{av}/P_0, 0.611
m_2/m_0, 0.982

(b) 23-Percent-solidity screen.

Figure 13. - Continued. Effect of internal screens on total-pressure contours at primary rake. Short diffuser model; screens located at model station 14.28.

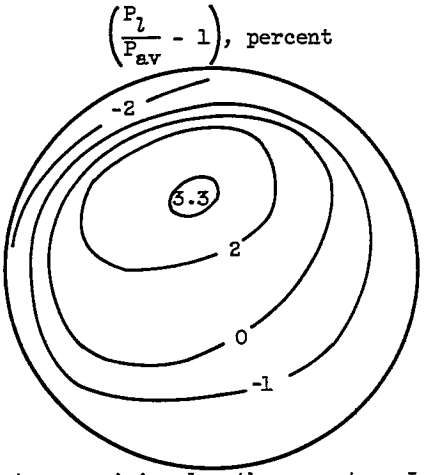

Constant-area mixing-length parameter, L/D, 0.46
Rake Mach number, 0.204
Total-pressure distortion, $\Delta P/P_{av}$, 5.3 percent
Total-pressure recovery, P_{av}/P_0, 0.597
Inlet mass-flow ratio, m_2/m_0, 0.978

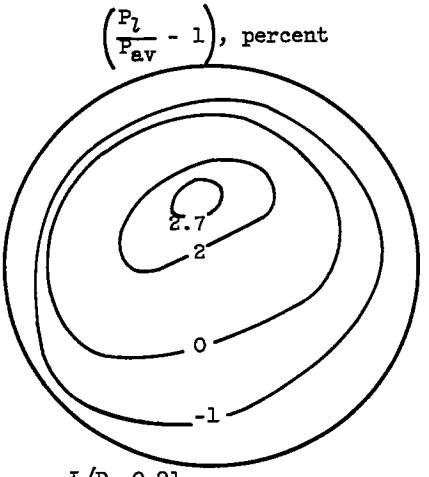

L/D, 0.91
Rake Mach number, 0.201
$\Delta P/P_{av}$, 4.5 percent
P_{av}/P_0, 0.597
m_2/m_0, 0.966

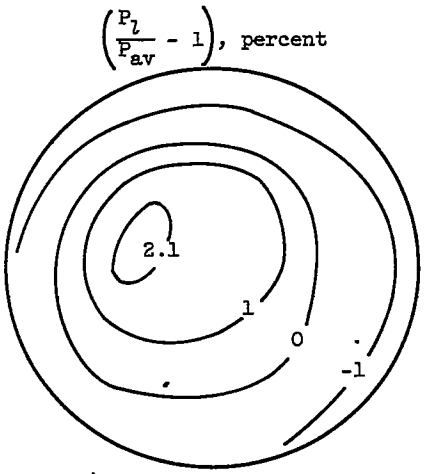

L/D, 1.82
Rake Mach number, 0.203
$\Delta P/P_{av}$, 3.9 percent
P_{av}/P_0, 0.599
m_2/m_0, 0.975

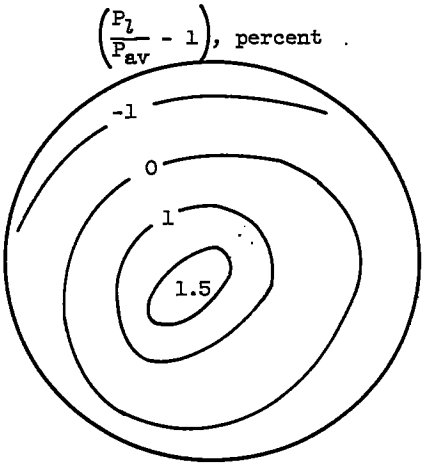

L/D, 3.50
Rake Mach number, 0.203
$\Delta P/P_{av}$, 2.7 percent
P_{av}/P_0, 0.600
m_2/m_0, 0.977

(c) 40-Percent-solidity screen.

Figure 13. - Concluded. Effect of internal screens on total-pressure contours at primary rake. Short diffuser model; screens located at model station 14.28.

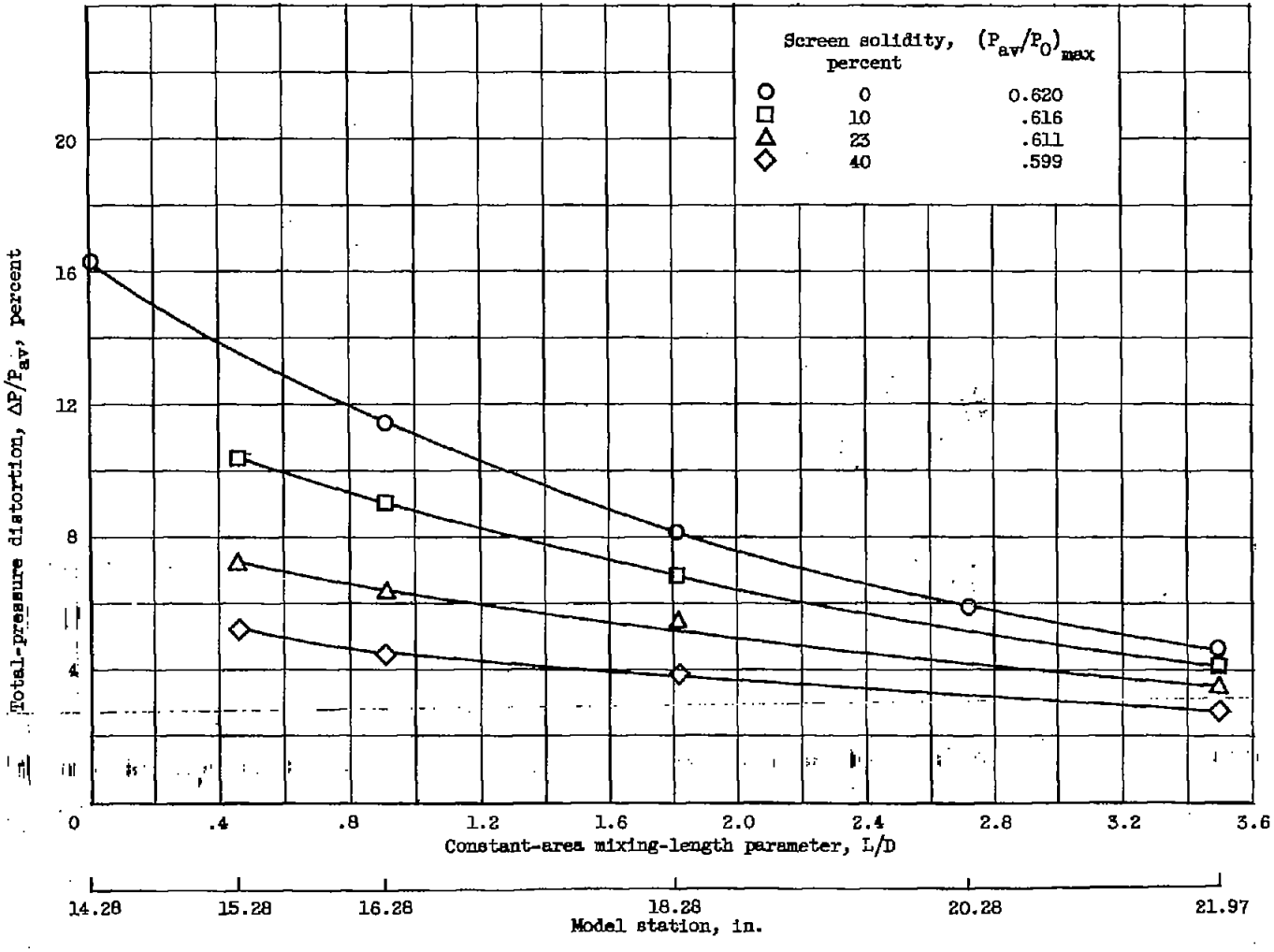

(a) Short diffuser; screens located at model station 14.28.

Figure 14. - Effect of screens and mixing length on total-pressure distortion.

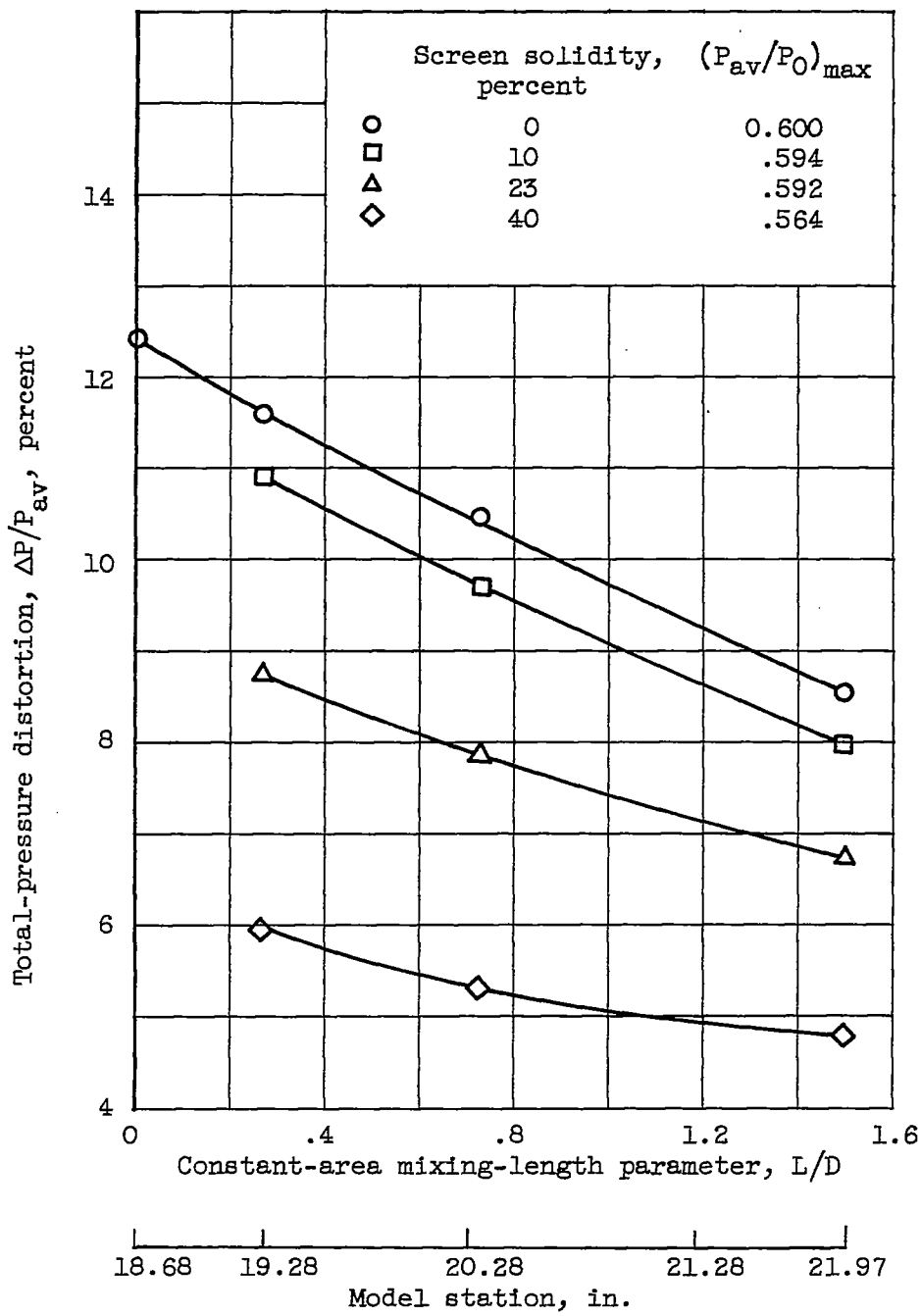

(b) Long diffuser; screens located at model station 14.85.

Figure 14. - Concluded. Effect of screens and mixing length on total-pressure distortion.

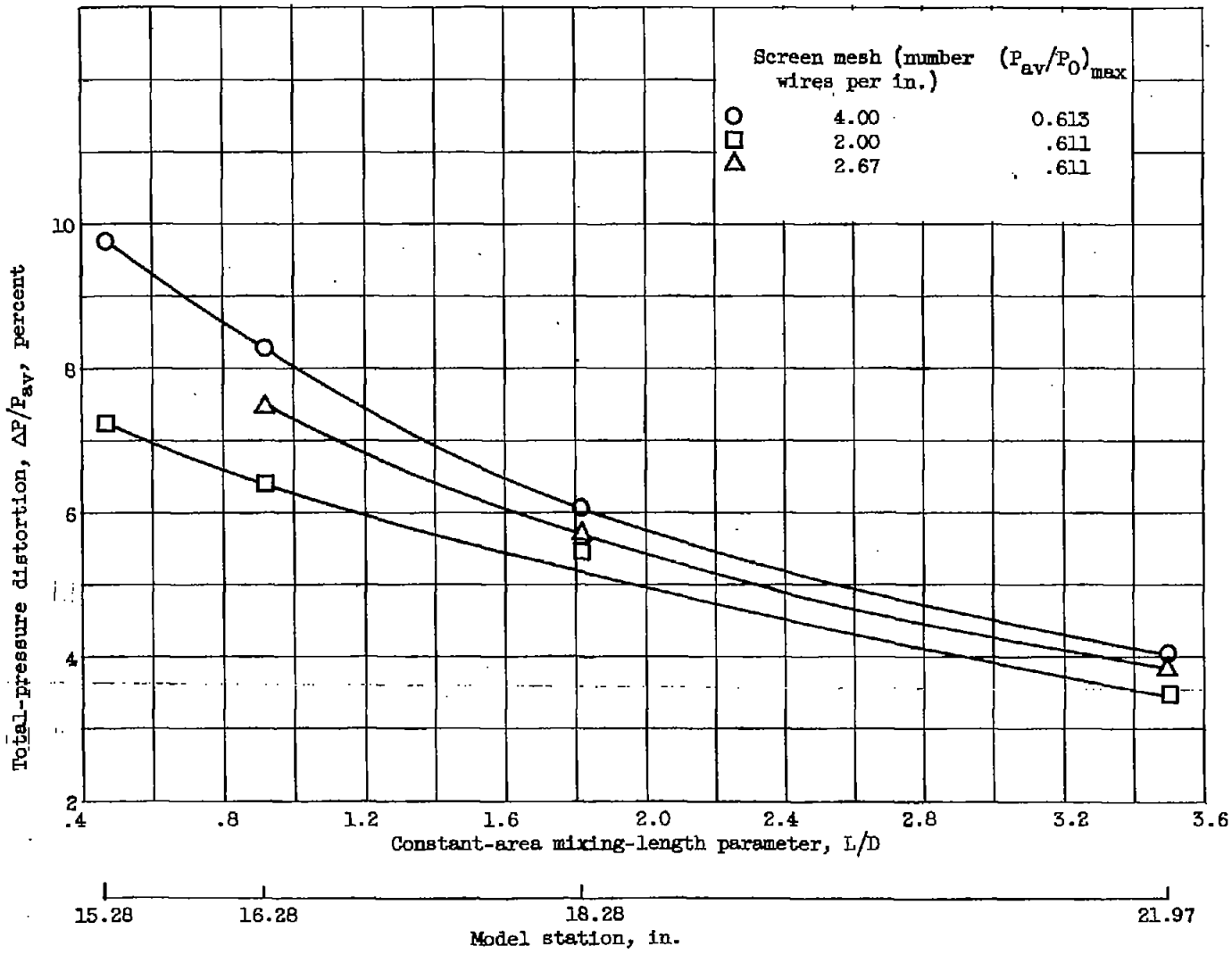

Figure 15. - Effect of screen mesh on distortion. Screen solidity, 23 percent; screens located at model station 14.28; short diffuser.

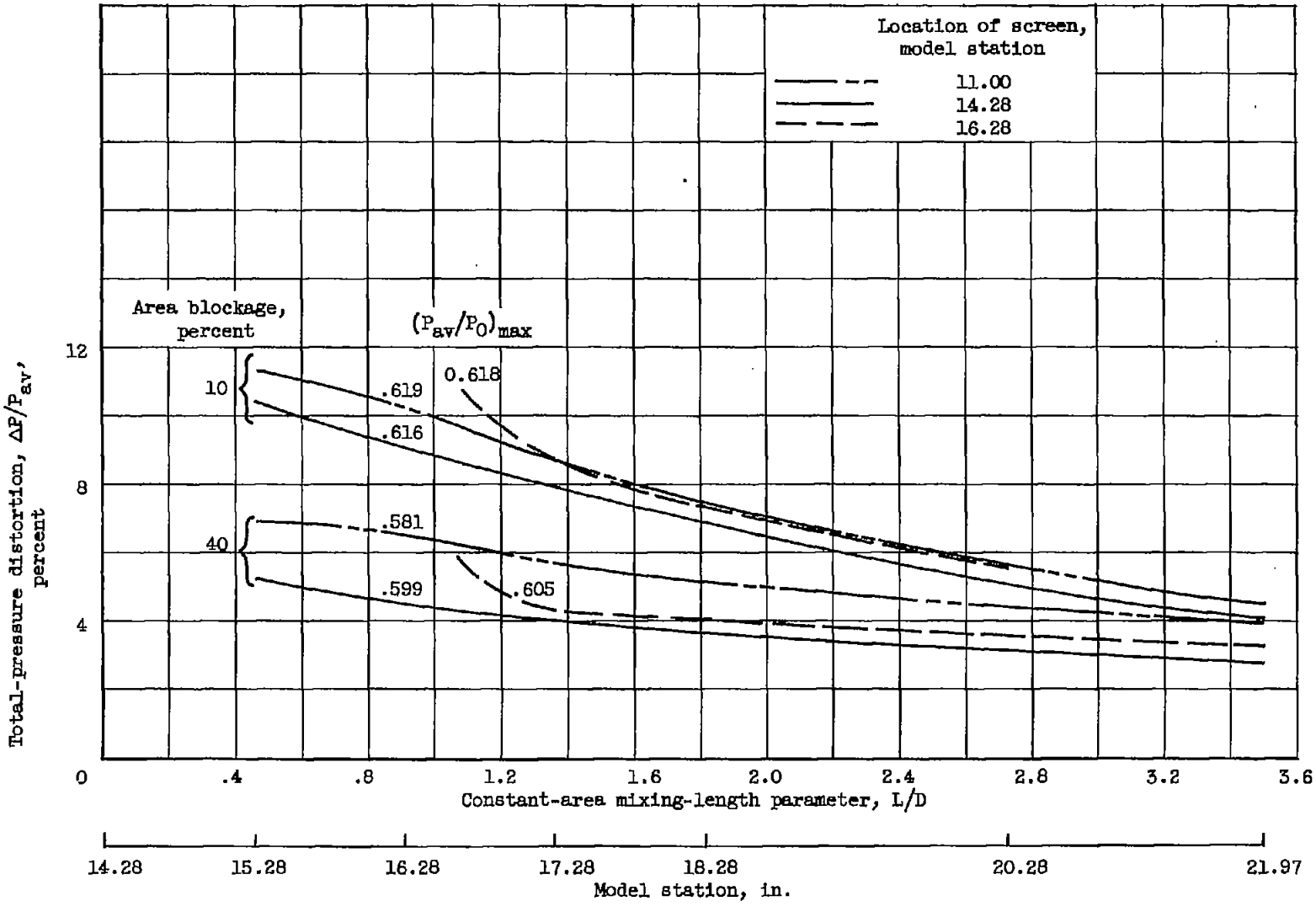

Figure 16. - Effect of screen location on total-pressure distortion. Short diffuser model.

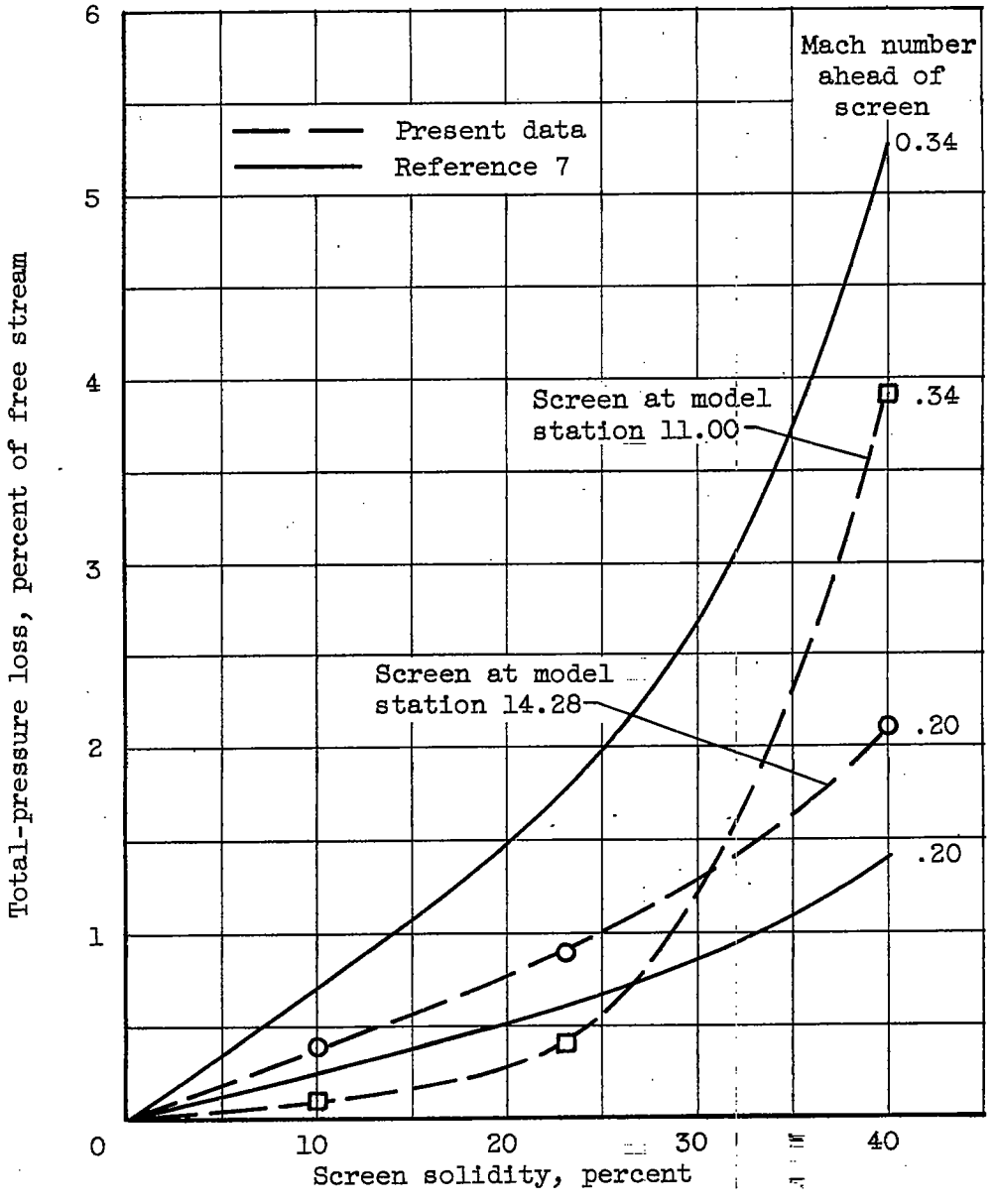

Figure 17. - Reduction of maximum pressure recovery due to screen losses.

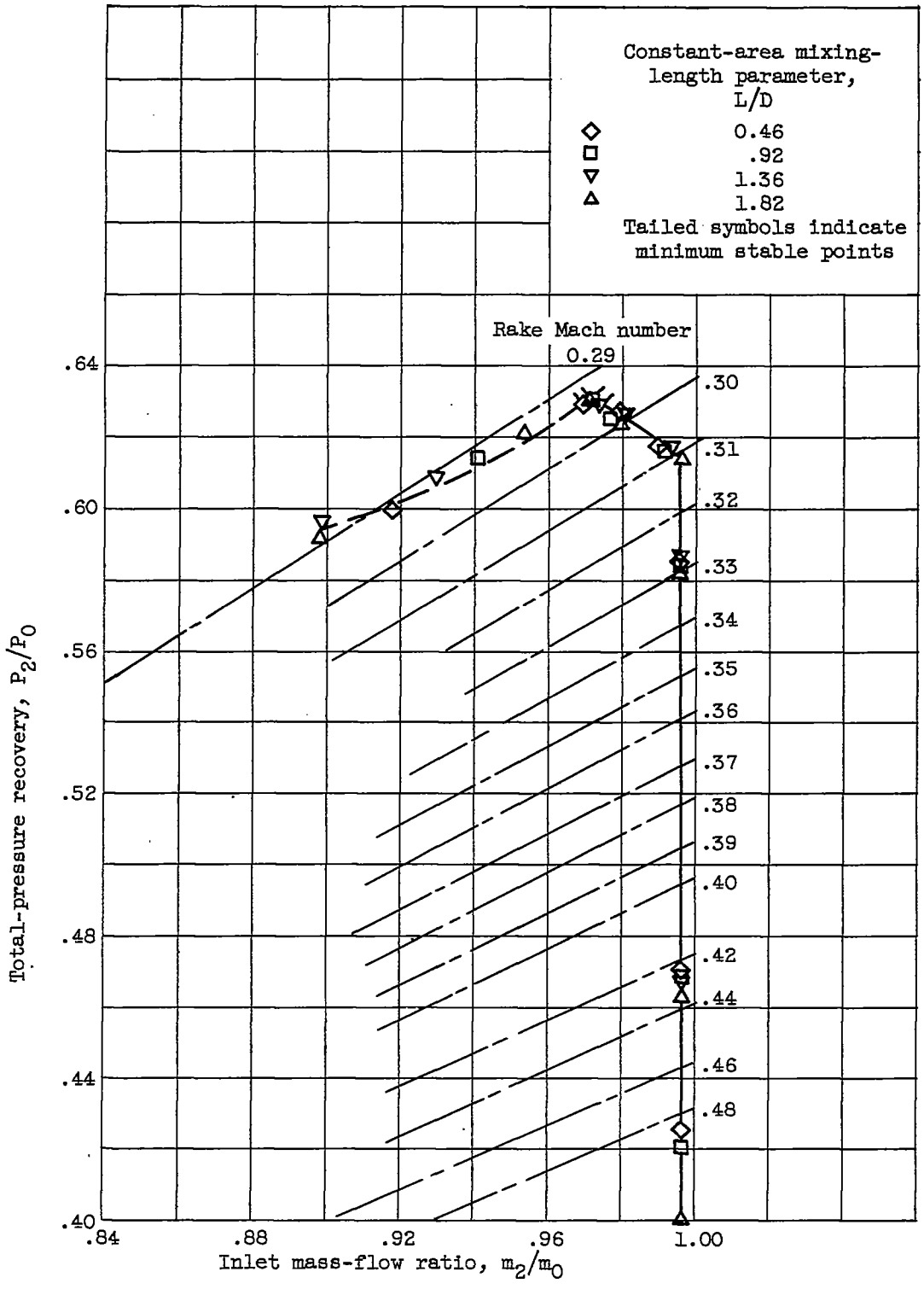

Figure 18. - Performance of short diffuser model with contracting section.

$\left(\frac{P_l}{P_{av}} - 1\right)$, percent

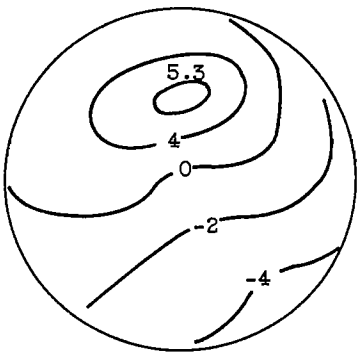

Constant-area mixing-length parameter, L/D, 0.46
Rake Mach number, 0.294
Total-pressure distortion, $\Delta P/P_{av}$, 9.7 percent
Total-pressure recovery, P_{av}/P_0, 0.628
Inlet mass-flow ratio, m_2/m_0, 0.970

$\left(\frac{P_l}{P_{av}} - 1\right)$, percent

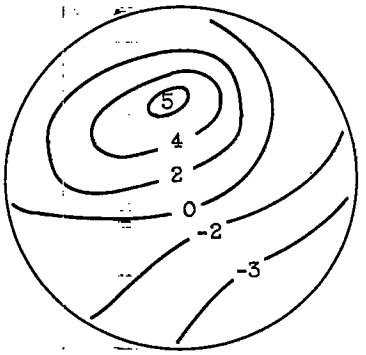

L/D, 0.92
Rake Mach number, 0.294
$\Delta P/P_{av}$, 8.4 percent
P_{av}/P_0, 0.630
m_2/m_0, 0.972

$\left(\frac{P_l}{P_{av}} - 1\right)$, percent

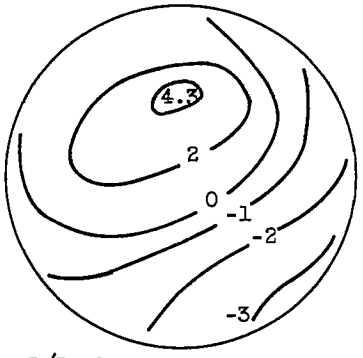

L/D, 1.36
Rake Mach number, 0.205
$\Delta P/P_{av}$, 7.3 percent
P_{av}/P_0, 0.628
m_2/m_0, 0.974

$\left(\frac{P_l}{P_{av}} - 1\right)$, percent

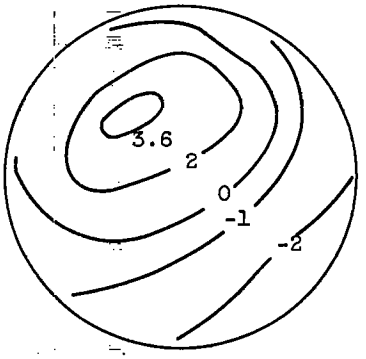

L/D, 1.82
Rake Mach number, 0.294
$\Delta P/P_{av}$, 6.3 percent
P_{av}/P_0, 0.630
m_2/m_0, 0.972

Figure 19. - Total-pressure contours at primary rake. Short diffuser model with contracting section.

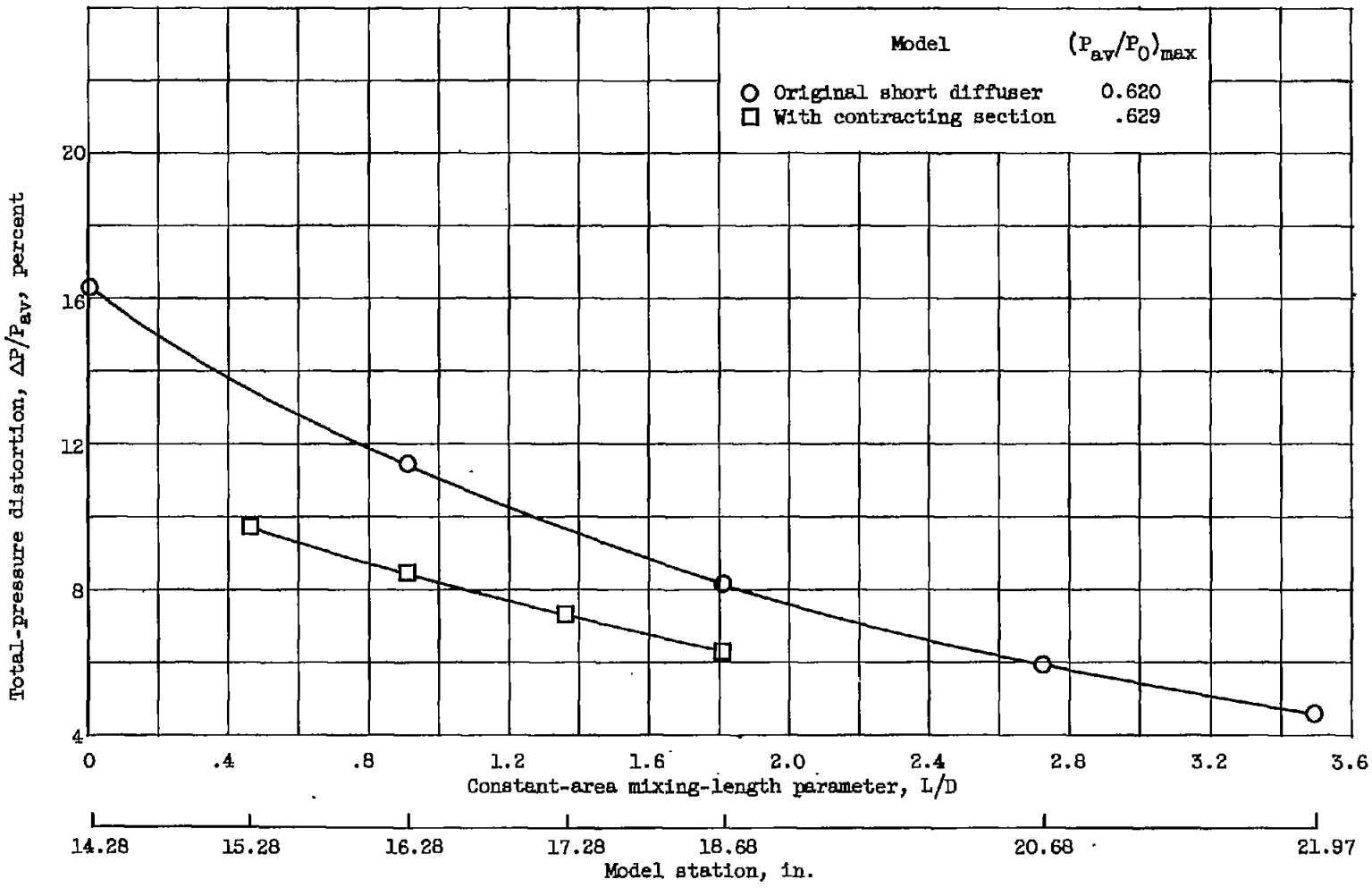

Figure 20. - Effect of contraction section on total-pressure distortion. Short diffuser model.

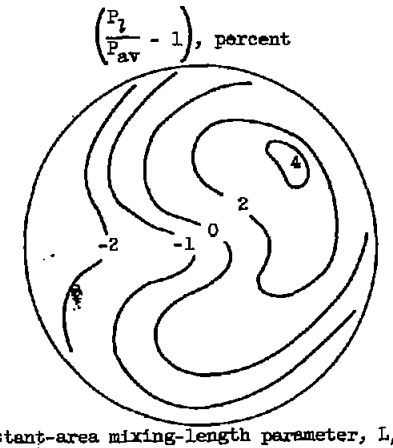

Constant-area mixing-length parameter, L/D, 0
Rake Mach number, 0.211
Total-pressure distortion, $\Delta P/P_{av}$, 6.7 percent
Total-pressure recovery, P_{av}/P_0, 0.579
Inlet mass-flow ratio, m_2/m_0, 0.982

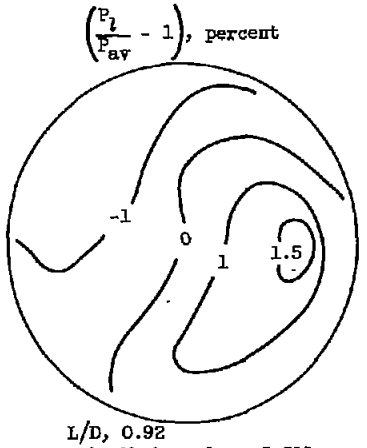

L/D, 0.92
Rake Mach number, 0.211
$\Delta P/P_{av}$, 3.4 percent
P_{av}/P_0, 0.582
m_2/m_0, 0.985

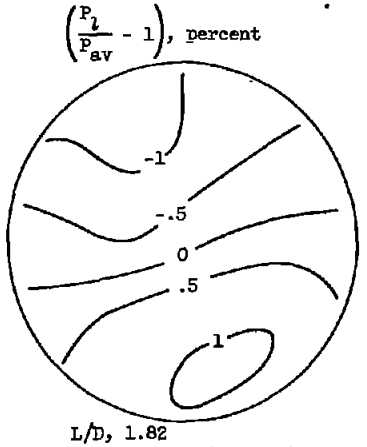

L/D, 1.82
Rake Mach number, 0.212
$\Delta P/P_{av}$, 2.2 percent
P_{av}/P_0, 0.578
m_2/m_0, 0.985

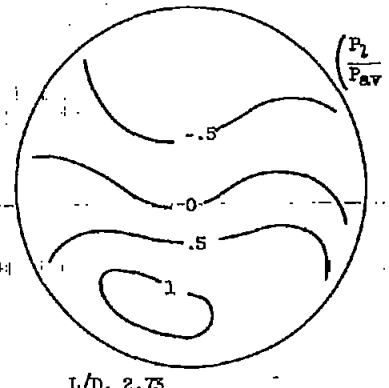

L/D, 2.73
Rake Mach number, 0.212
$\Delta P/P_{av}$, 2.0 percent
P_{av}/P_0, 0.579
m_2/m_0, 0.985

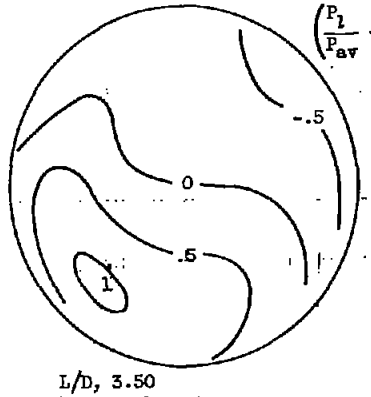

L/D, 3.50
Rake Mach number, 0.213
$\Delta P/P_{av}$, 1.6 percent
P_{av}/P_0, 0.577
m_2/m_0, 0.986

Figure 21. - Total-pressure contours at primary rake. Short diffuser model with raised centerbody.

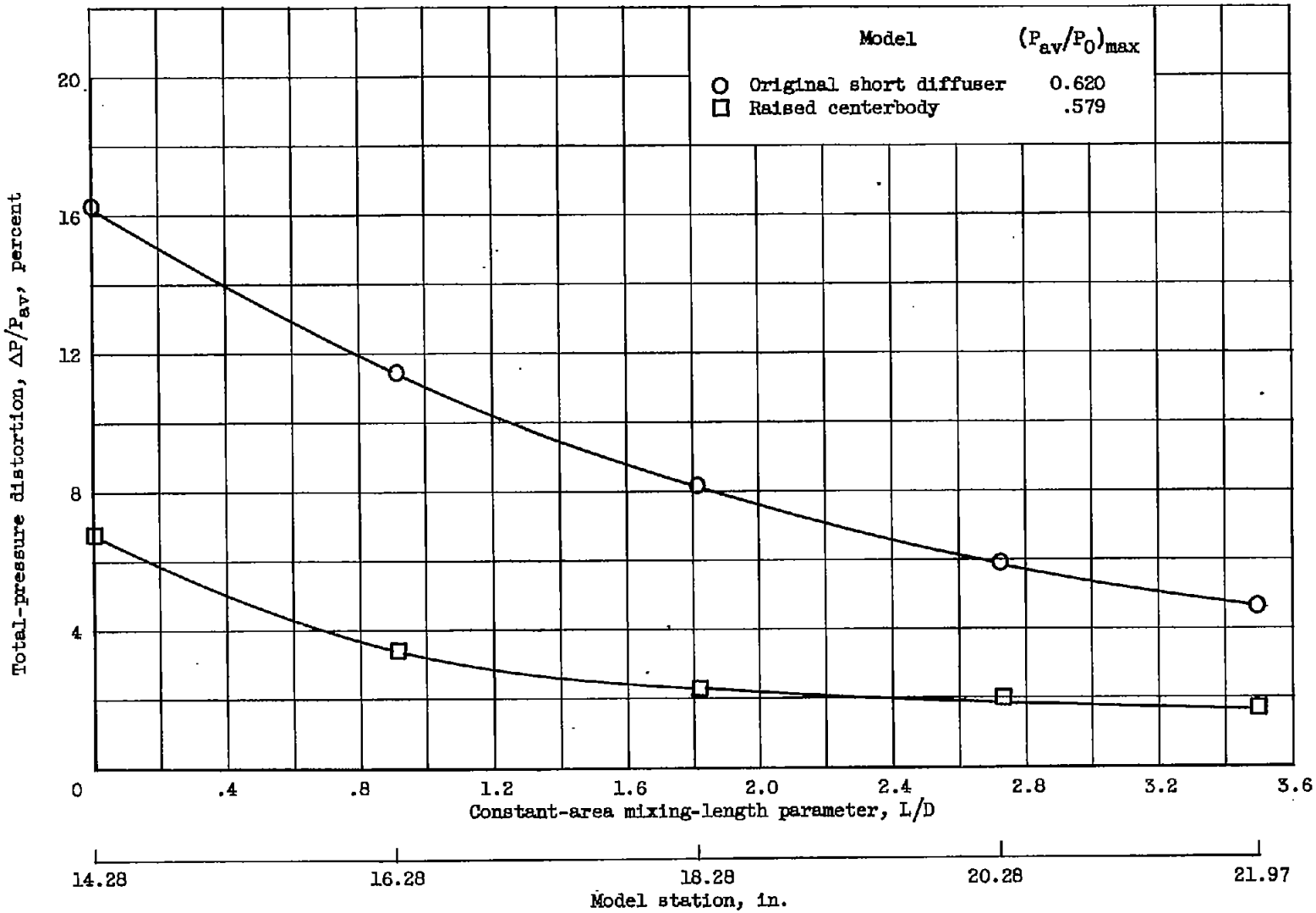

Figure 22. - Effect of raising centerbody on total-pressure distortion. Short diffuser model.

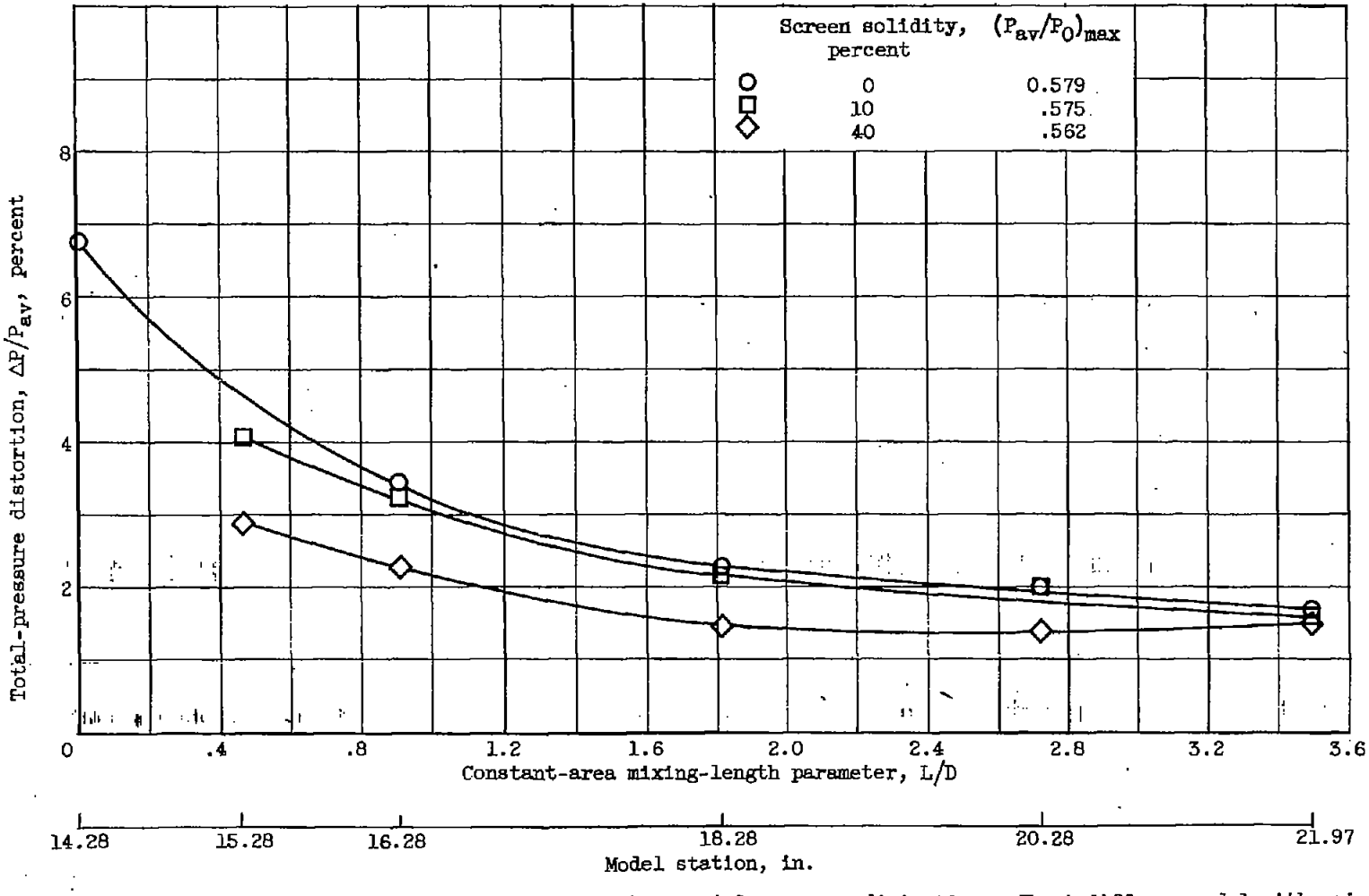

Figure 23. - Effect of screens and mixing length on total-pressure distortion. Short diffuser model with raised centerbody.

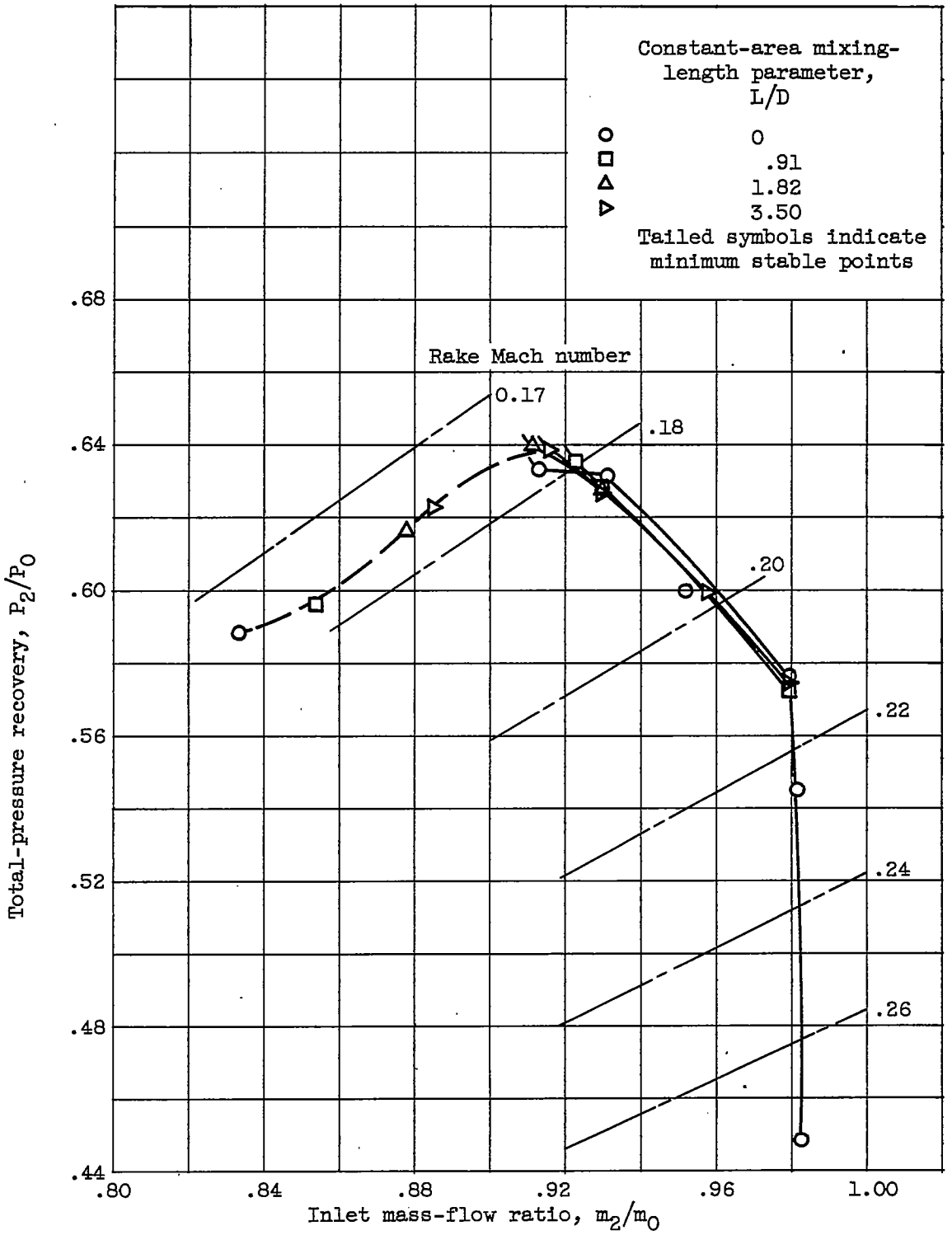

Figure 24. - Inlet performance with internal bleed. Short diffuser model.

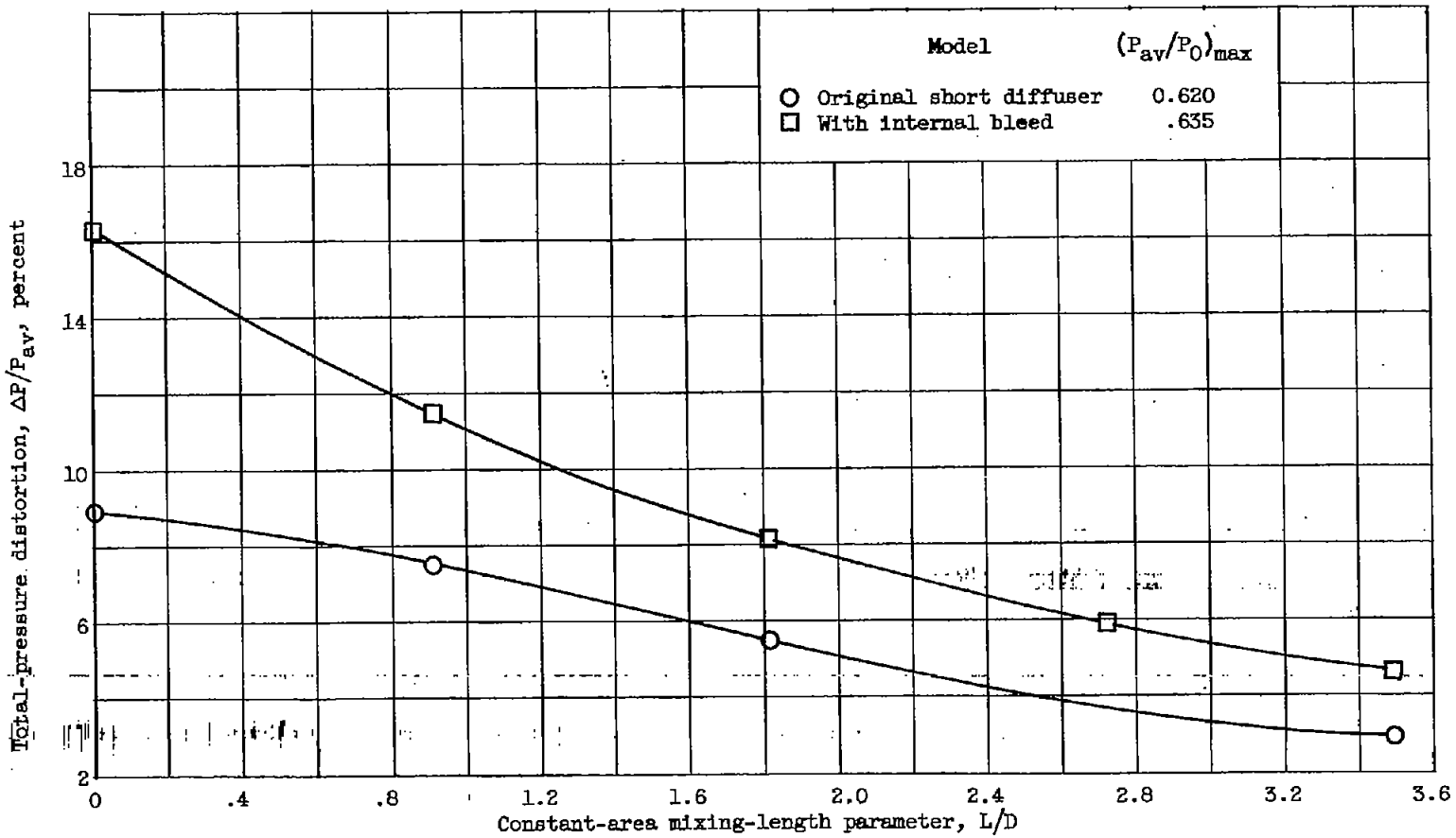

Figure 25. - Effect of internal bleed on total-pressure distortion. Short diffuser model.